HHS Public Access

Author manuscript

Acta Biomater. Author manuscript; available in PMC 2021 December 28.

Published in final edited form as:

Acta Biomater. 2020 January 15; 102: 231–246. doi:10.1016/j.actbio.2019.11.029.

Functional Role of Glycosaminoglycans in Decellularized Lung Extracellular Matrix

Franziska E. Uhl, PhD[1,2], **Fuming Zhang, PhD**[3], **Robert A. Pouliot, PhD**[1], **Juan J. Uriarte, PhD**[1], **Sara Rolandsson Enes, PhD**[1,2], **Xiaorui Han**[3], **Yilan Ouyang**[3], **Ke Xia, PhD**[3], **Gunilla Westergren-Thorsson, MD PhD**[2], **Anders Malmström, PhD**[2], **Oskar Hallgren, PhD**[2], **Robert J. Linhardt, PhD**[3], **Daniel J. Weiss**[*,1]

[1]University of Vermont, Larner College of Medicine, Burlington, VT, USA

[2]Lund University, Department of Experimental Medical Science, Faculty of Medicine, Lund University, Lund, Sweden

[3]Center for Biotechnology and Interdisciplinary Studies, Rensselaer Polytechnic Institute, Troy NY, USA

Abstract

Despite progress in use of decellularized lung scaffolds in *ex vivo* lung bioengineering schemes, including use of gels and other materials derived from the scaffolds, the detailed composition and functional role of extracellular matrix (ECM) proteoglycans (PGs) and their glycosaminoglycan (GAG) chains remaining in decellularized lungs, is poorly understood. Using a commonly utilized detergent-based decellularization approach in human autopsy lungs resulted in disproportionate losses of GAGs with depletion of chondroitin sulfate/dermatan sulfate (CS/DS) > heparan sulfate (HS) > hyaluronic acid (HA). Specific changes in disaccharide composition of remaining GAGs were observed with disproportionate loss of NS and NS2S for HS groups and of 4S for CS/DS groups. No significant influence of smoking history, sex, time to autopsy, or age was observed in native vs. decellularized lungs. Notably, surface plasmon resonance demonstrated that GAGs remaining in decellularized lungs were unable to bind key matrix-associated growth factors FGF2, HGF, and TGFβ1. Growth of lung epithelial, pulmonary vascular, and stromal cells cultured on

[*]Corresponding Author Daniel J. Weiss MD PhD, University of Vermont, Larner College of Medicine, 149 Beaumont Avenue, Health Science Research Facility (HSRF) 226, Burlington, VT 05405, USA, daniel.weiss@uvm.edu, fax number: +1 802-847-2444.

Disclosures:

Author contributions:

All authors have approved the final article and helped with analysis and interpretation of data.

All authors have read, edited, and approved the final manuscript.

FEU, ZH, RAP, JJU, SRE, XH, YO, KX, OH have conducted experiments and analyzed data.

FEU, ZH, RAP, RJL, DJW conceptualized the studies.

FEU, DJW wrote the original manuscript.

Declaration of interest:

No author has competing interests

Data availability

The raw/processed data required to reproduce these findings cannot be shared at this time due to technical or time limitations.

the surface of or embedded within gels derived from decellularized human lungs was differentially and combinatorially enhanced by replenishing specific GAGs and FGF2, HGF, and TGFβ1. In summary, lung decellularization results in loss and/or dysfunction of specific GAGs or side chains significantly affecting matrix-associated growth factor binding and lung cell metabolism. GAG and matrix-associated growth factor replenishment thus needs to be incorporated into schemes for investigations utilizing gels and other materials produced from decellularized human lungs.

Keywords

lung; decellularization; glycosaminoglycan; matrix-associated growth factors; COPD; extracellular matrix gel

Introduction

Decellularized lungs and materials derived from these, including gels and bioinks, are increasingly being utilized in studies of lung regenerative engineering. However, a significant under-investigated area is the content and function of the remaining glycosaminoglycans (GAGs) in decellularized lung extracellular matrix (ECM) scaffolds. Most GAGs are cell-associated and removed during decellularization. However, it is likely that GAGs associated with the ECM scaffold of the decellularized lungs have critical impact on the behavior and proper functioning of the cells seeded directly into the decellularized lungs or into derivative gels produced from them [1, 2]. While progress is being made with respect to the role of different ECM proteins such as collagen, laminins, tenascin C, and others [3–7] on cell behaviors, the roles of the remaining proteoglycans (PGs) and glycosaminoglycans (GAG) in the decellularized lung ECM scaffolds are less well understood [8, 9].

GAGs in particular are implicated as important directors of ECM assembly, organization, and remodeling during homeostasis and normal repair processes [4]. Cell-ECM interactions facilitated by GAGs can further direct cell behavior by sequestration and presentation of bioactive molecules such as growth factors, by direct interaction with cell membrane receptors, and as anchor sites for cells to recognize or attach to the local ECM architecture. These properties allow GAGs to play critical roles in cell growth, differentiation, and function [4, 7]. However, limited information exists with respect to the content, structure, and function of specific GAGs remaining in decellularized lung ECM, particularly with respect to the different classes of GAG chain modifications resulting in the different functional groups of major sulfated GAG classes heparan sulfate (HS), chondroitin sulfate (CS), and dermatan sulfate (DS) and for hyaluronic acid (HA). This includes both direct roles of these GAGs on cell behaviors as well as binding and activation by specific HS, CS, DS, and HA functional groups of matrix-associated growth factors such as transforming growth factor beta (TGFβ1), fibroblast growth factor 2 (FGF2), and hepatocyte growth factor (HGF), each of which play significant roles in cell lung behaviors, [10–12]. Understanding the role of both matrix-associated growth factor-dependent and -independent actions of GAGs remaining in decellularized lung materials will provide critical new information that will increase the likelihood of successful use of derivative materials such

as gels and bioinks as well as the whole scaffolds themselves in lung bioengineering schemes. Additionally, better understanding of decellularized ECM GAGs in diseased lungs, for example in emphysema (chronic obstructive pulmonary disease, COPD) or idiopathic pulmonary fibrosis (IPF), will provide further insights in disease pathogenesis and provide potential new therapeutic approaches [1, 13].

We therefore systematically assessed GAG content and function in decellularized human lungs obtained from autopsy. This included lungs from patients with no history or clinical evidence of lung disease as well as lungs from patients with documented COPD. Notably, differential loss of specific major GAG classes HS, CS, DS, and HA as well as differential loss of GAG entities with specific modifications in these classes was observed as was the ability of GAGs isolated from the decellularized lungs to bind key matrix-associated growth factors FGF2, HGF, and TGFβ1. Functionally, this had significant effects on growth of lung epithelial, pulmonary vascular, and fibroblast cells grown either in or on decellularized human lung ECM gels wherein systematic addition of selected GAGs and matrix-associated growth factors to the gels had differential and combinatorial effects on cell growth. Notably, there were different effects of the GAGs and growth factors depending on whether the cells were cultured on top of or embedded within the gels. This provides strong and unique evidence that GAGs are both selectively depleted and functionally altered in decellularized human lungs and materials derived from them. Further, the model system utilized can influence the effect of replenishing GAGs and matrix-associated growth factors. Continued exploration of GAGs and matrix-associated growth factors must be considered for better understanding the biology of decellularized lung scaffolds and in lung recellularization schemes as well as in investigations of materials produced from decellularized lungs.

Materials and Methods

Human lungs

Human lungs were obtained from the University of Vermont (UVM) autopsy services under appropriate institutional guidelines. Lungs were categorized into those from lifelong non-smokers, former (remote) smokers, or current smokers/patients with clinical/radiographic COPD based on available medical records.

Decellularization

Lungs were decellularized using sequential perfusion with phosphate buffered saline (PBS, Corning), deionized water, Triton-X 100 (Sigma), sodium deoxycholate (Sigma), porcine pancreatic DNAse (Sigma), and peracetic acid (PAA, Sigma) through both the vasculature and airways at a constant flow rate as previously described [14]. A more detailed protocol is available in the appendix to this article. Adequacy of decellularization was assessed by microscopic examination of Hematoxylin & Eosin (H&E) stained, mounted, 5 μm thick paraformaldehyde-fixed paraffin sections, and by measurement of residual double stranded DNA as previously described [13, 15].

Characterization of residual matrix-associated growth factors in decellularized lungs

Native and decellularized lung tissue, three samples per lung, were analyzed by semi-quantitative LC-MS utilizing a QExactive mass spectrometer (Thermo Fisher Scientific) as previously utilized at the UVM Proteomics Core Facility [13, 15, 16]. Spectra were searched against existing protein sequence databases compiled from UniProtKB/Swiss Prot database (http://www.uniprot.org) using the Proteome Discoverer software (version 1.4.1.14; Thermo Electron, San Jose, CA, USA). Proteins positively identified with two or more distinct peptide hits were classified according to published matrisome and proteoglycan lists [17–19]. Identified proteins were compared using a Venn diagram (biovenn, http://www.biovenn.nl/index.php).

Characterization of specific anionic GAGs and disaccharide chains in decellularized lungs

Decellularized lung tissue was first digested with pronase and benzonase and GAGs isolated by anion exchange chromatography [9, 20]. This was followed by digestion of these polysaccharides with GAG lyases that specifically degrade HS: heparinase I, II and III; CS/DS and HA: chondroitinase ABC; or DS: chondroitinase B. The disaccharides were then labeled with the fluorophore, 2-aminoacridone (AMAC), and analyzed with fluorescence-HPLC [21]. Quantification of each disaccharide was done by comparison with known amounts of disaccharide standards [20, 21]. Three locations of each lung were evaluated and averaged. Principal component analysis (PCA) was utilized to compare the effect of tissue origin (native vs. decellularized), smoking status, disease state, age, gender, and time to autopsy before tissue curation and subsequent decelluarization and was conducted using R (https://www.r-project.org/).

Staining of GAGs

Immunohistochemistry was done as previously described [9]. Briefly, 10 μm cryosections of lung tissue from patients before or after decellularization were air-dried and rehydrated. To verify the specificity of the staining, tissue sections were pre-treated 1 h at 37°C with lyases. For HS; pretreatment was conducted with a combination of heparinase II (at 15 mU/section) and heparinase III (at 6 mU/section) (overexpressed in *E. coli*, a kind gift from Jian Liu, University of North Carolina at Chapel Hill) in an enzyme buffer made up of HEPES (20 mM), NaCl (50 mM), $CaCl_2$ (4 mM), and BSA (0.01%) (pH 7.2) and for CS with chondroitinase ABC (chondroitin ABC lyase, C3667, Sigma-Aldrich, St. Louis, MO, USA) (5 mU/section) in 50 mM NH_4OAc and 0.1 mg/mL BSA. This was followed by endogenous peroxidase activity blocking in 3 % hydrogen peroxide for 10 min., followed by blocking in 1 % BSA in PBS-Tween-20 (0.05 %) for 20 min. Tissue sections were incubated with primary antibodies overnight at 4°C: anti-HS, 10E4 epitope (Amsbio, Abingdon, UK) at 1:300 and anti-CS, clone CS-56 (Sigma-Aldrich, St. Louis, MO, USA) at 1:400. After washing, the Envision + Dual Link system (Agilent, Santa Clara, CA, US) was used to visualize the staining with a 30 min incubation with HRP-labeled polymers followed by development with DAB and counterstaining with Mayer's haematoxylin (Sigma-Aldrich, St. Louis, MO, USA). Sections were dehydrated, mounted with Pertex mounting medium (Histolab, Gothenburg, Sweden) and photographed using a TE2000-E microscope (Nikon, Tokyo, Japan) equipped with a DXM1200C camera (Nikon, Tokyo, Japan).

Binding of representative matrix-associated growth factors by competitive interaction using surface plasmon resonance (SPR)

The binding of the matrix-associated growth factors FGF2 (Amgen), TGFβ1 (R&D systems, Minneapolis, MN), and HGF (Gibco Life Technology, Gaithersburg, MD) to heparin and to GAGs isolated from native and decellularized lung tissue was analyzed using Sensor streptavidin (SA) chips (GE Healthcare Life Sciences, Pittsburgh, PA) [22]. All of these matrix-associated growth factors have significant effects on lung development and repair from injury [4, 7]. To isolate the GAGs, native and decellularized lung samples were treated with 10 mL acetone for 30 min and digested by Actinase E (Kaken Pharmaceutical, Tokyo, Japan, 10 mg/mL) at 55°C until all the tissue was dissolved (about 36 h). Total GAGs were purified using Maxi Q spin columns (Sartorius Stedim North America, Bohemia, NY). Recombinant heparin lyases I, II, III (pH optima 7.0−7.5) were used to isolate CS/DS from total GAGs and recombinant chondroitin lyase ABC (10 mU each, pH optimum 7.4) was used to isolate HS from total GAGs. Porcine intestinal heparin (16 kDa, Celsus Laboratories, Cincinnati, OH, USA), HS, or CS/DS (each 2 mg), and amine-PEG3-Biotin (2 mg, Pierce, Rockford, IL, USA) were dissolved in 8 M sodium cyanoborohydride ($NaCNBH_3$, Sigma) and incubated at 70°C for 24 h. By addition of $NaCNBH_3$ the concentration was increased to 16 M and the solution incubated for another 24 h at 70°C. After cooling to room temperature, the mixture was desalted using spin columns (3,000 MWCO, Millipore (Burlington, MA). Biotinylated GAGs were collected, freeze-dried, and immobilized to Sensor SA chips based on the manufacturer's protocol. In brief, 20 μL solution of the HS-biotin and CS/DS-biotin conjugate (0.1 mg/mL) in HBS-EP running buffer (0.01 M HEPES, 0.15 M NaCl, 3 mM EDTA, 0.005% surfactant P20, pH 7.4) was injected over flow cell 2 (FC2) and 3 (FC3) of the SA chip at a flow rate of 10 μL/min, respectively. The successful immobilization of GAGs was confirmed by the observation of a ~200 to 400 resonance unit (RU) increase in the sensor chip. Flow cell 4 (FC4) was immobilized with biotinylated heparin as positive control. The control flow cell (FC1) was prepared by 1 min injection with saturated biotin as negative. The matrix-associated growth factor samples were diluted in HBS-EP buffer (0.01 M HEPES, 0.15 M NaCl, 3 mM EDTA, 0.005% surfactant P20, pH 7.4). Different dilutions of matrix-associated growth factor samples were injected at a flow rate of 40 μL/min. At the end of the sample injection, the same buffer was flowed over the sensor surface to facilitate dissociation. After a 3 min dissociation time, the sensor surface was regenerated by injecting with 40 μL of 2 M NaCl to fully regenerate the surface. The response was monitored as a function of time (sensorgram) at 25°C on a BIAcore 3000 (using BIAcore 3000 control and BIAevaluation software, version 4.0.1).

Cell culture

Cells were routinely cultured in cell-specific culture medium in tissue-culture-treated plastic in an incubator at 37°C and 5% CO_2. Human bronchial epithelial cells (HBE-135-E6E7, ATCC, CRL-2741) were cultivated in keratinocyte-serum free medium (Gibco) with 5 ng/mL human recombinant epidermal growth factor (EGF, Gibco), 0.05 mg/mL bovine pituitary extract (Gibco), 0.005 mg/mL insulin (Sigma), 500 ng/mL hydrocortisone (Sigma), and 1% Penicillin, Streptomycin (Gibco) and not used past passage 15. Primary human pulmonary vascular endothelial cells (CBF, courtesy of Dr. Mervin Yoder, Indiana University) were cultivated in endothelial medium (VascuLife® VEGF Endothelial Medium

Complete Kit, Lifeline Cell Technology) and expanded on collagen type I coated plates. Plates were pre-coated with sterile 50-μg/mL rat tail collagen type I (Corning) in 0.02 M acetic acid (Sigma) in an incubator for at least 1 h. Plates were washed with 1X PBS before cell seeding and CBF cells were not used past passage 15. Human lung fibroblasts (HLF, CCD-19Lu, ATCC) were cultivated in Eagle's Minimum Essential Medium (Gibco), supplemented with 10% fetal bovine serum (FBS, Hyclone) and 100 IU/mL penicillin/100 mg/mL streptomycin (Corning) and not used past passage 10.

Effect of soluble GAGs and matrix-associated growth factors on cell metabolic activity

CBF and HLF cells were seeded at 2,000 cells per 96-well, HBE cells were seeded at 5,000 cells per 96-well and attached overnight (about 17 h). Growth media were subsequently changed to media containing either HS (from porcine intestinal mucosa, Celsus Laboratories (Cincinnati, OH)), CSA (from bovine trachea, Sigma, St. Louis, MO) as representative for chondroitin sulfates, or DS (isolated from pig skin at Lund University) with or without the addition of different matrix-associated growth factors: TGFβ1 (R&D Systems), FGF2 (Gibco), and HGF (Gibco) at a concentration of 5 ng/mL for TGF and FGF2 and 25 ng/mL for HGF. Matrix-associated growth factor concentrations utilized were based on literature references for effective amounts needed to affect cell growth [23]. GAGs were added at concentrations ranging from 0.001–10 μM. Calculation of the concentration was based on the average molecular weight of each GAG. 10% Triton X-100 served as negative control, pure cultivation medium as positive control. Cell phenotype was assessed using bright field imaging. Assessment of metabolic activity utilizing Alamar Blue was used as a surrogate measure of cell growth as per manufacturer's instructions. After cultivation for 1, 3, 5, or 7 days cells were incubated with 200 μL medium containing 100 μL/mL Alamar Blue (Thermo Scientific) for 1–3 h accounting for the different cell numbers and metabolic activities on each day of cultivation. 150 μL of supernatant was transferred into a new 96-well plate and fluorescence measured at 530/25 nm excitation and 590/35 nm emission with subtraction of background fluorescence of Alamar Blue containing medium without cells. Data was displayed as fluorescence relative to fluorescence of cells in the control medium without GAGs. 4–5 wells per condition were evaluated in each of at least 3 replicate experiments. Media was changed every other day with fresh matrix-associated growth factor added to the media change.

Preparation of ECM gels for Cell Experiments

Two different types of gels were prepared from a pre-gel solution to test the effect of GAGs on cell viability and proliferation: a) pure collagen I gels (Col1) and b) decellularized human lung ECM/type I collagen reinforced gels (Col1/ECM). Pure collagen gels were prepared using commercially available rat-tail collagen I (Corning), shipped at 3.54 – 3.90 mg/mL in 20 mM acetic acid. For creating gels from decellularized human lung ECM the PAA step and storage solution were not utilized as this was found to negatively affect the gelation capabilities of the decellularized human ECM. Soluble lung derived ECM was prepared as previously described [26], briefly decellularized human lungs were dissected, frozen, lyophilized, and processed into a fine powder using a liquid nitrogen mill (Freezer Mill, Spex). Human lung-ECM powder was suspended at 10 mg/mL in enzymatic digestion

solution (1 mg/mL pepsin in 0.01M HCl), and solubilized for 72 h at room temperature, under constant agitation.

Undigested powder and insoluble particles were removed via centrifugation (10,000 RCF, 20 min) and the soluble human lung ECM supernatant was collected, neutralized to a pH of 7.0 (using sterile 0.1M NaOH), frozen at −80 °C, and lyophilized. Pre-solubilized ECM lyophilate was re-suspended in sterile-filtered 20 mM acetic acid on ice to a final concentration of 15 mg/mL. ECM/ type I collagen solutions were prepared by mixing the soluble human lung ECM (15 mg/mL) with type I collagen (3.54 – 3.9 mg/mL in 20 mM acetic acid) at a 1:3 ratio on-ice. To prepare the pre-gel solution, pure type I collagen (a) and human lung ECM/type I collagen solutions (b) were neutralized on ice with ice-cold 0.1 M NaOH and ice-cold 10X PBS, to reach pH 7.4. The pure type I collagen pre-gel solution (a), had a final concentration of 2.6–2.9-mg/mL, and the human lung ECM/type I collagen hybrid gels had a final concentration of 2.8 mg/mL soluble ECM and 2.2 mg/mL type I collagen. Both of these neutralized pre-gel solutions formed robust gels if incubated at 37ºC for at least 1 h.

Assessing the effect of GAGs and matrix-associated growth factors on cell growth and metabolic activity when seeded onto, or encapsulated within, a type I collagen or hybrid decellularized human ECM/type I collagen gel

All gel experiments were conducted in 96-well tissue culture plates with 50 μL pre-gel solution per well. To prepare gels containing GAGs, 1 μM soluble GAG stocks (HS, CSA, or DS) were diluted in pre-gel solution at 4°C to a final concentration of 0.1, 1, or 5 μM. For all experiments assessing the effect of GAG and matrix-associated growth factors on cell growth and metabolic activity, GAGs were diluted to a final concentration of 5 μM. When preparing gels to assess cells grown on top of the gels, the GAG pre-gel solution was first incubated to induce gelation and then the surface of the gels was treated with a growth factor solution overnight (5 ng/mL for TGFβ1 and FGF2, 25 ng/mL for HGF). Immediately prior to starting the experiment, the growth factor solution was aspirated, and the gels washed once with cultivation medium. 2,000 CBF, 2,000 HLF, or 5,000 HBE cells per well were seeded and incubated on top of the gels in 150 μL media per well. When preparing gels for cell encapsulation experiments the growth factors were added to the pre-gel solution along with the GAGs to the desired final concentration (5 ng/mL for TGFβ1 and FGF2, 25 ng/mL for HGF). Cells were counted, centrifuged, and re-suspended in the premixed pre-gel solutions, so that the resulting gels would contain 2,000 CBF, 2,000 HLF, or 5,000 HBE cells per well (50 μL gel-cell solution/well). Each gel was incubated for 1h to induce gelation and then 150 μL of cell media was added to each well.

For each experiment, media was changed every other day without addition of fresh matrix-associated growth factors in order to purely investigate the effect of the bound matrix-associated growth factors. The Alamar Blue assay was used to determine metabolic activity, as a surrogate for cell growth, on days 3, 5, and 7. Cell viability and phenotype was additionally assessed using live-dead staining (Molecular Probes) according to the manufacturer’s instructions and fluorescent imaging on day 8 of culture. Four gels were

seeded per experiment for each condition in three individual experiments each for either collagen-only or mixed decellularized human lung ECM/type I collagen gels.

Statistical analyses

Data is displayed as mean ± standard deviation (SD) or box plots with whiskers (Tukey). GAG quantification data is shown as paired plots matching native and decellularized tissue from each lung. The analytical variability for GAG disaccharide analysis is <3% [20, 21]. Comparison between control and experimental conditions was done by one sample t-test against a fixed value, Students' t-test, and One- or Two-way ANOVA. Results were considered significant at $p<0.05$ [13, 16, 21].

Results

For the lungs obtained at autopsy, patient demographics are depicted in Table 1 with a more summarized overview shown in Table 2. The mean age of non-COPD and COPD patients was comparable while there was a non-significant trend towards lower time to autopsy in the ex-smokers and COPD patients compared to the non-smokers. The COPD and ex-smokers were predominantly male while the non-smokers were predominantly female. Two of the COPD patients were current smokers at the time of death. Appendix Table 1 shows the different studies for which each lung was utilized.

The matrisome composition of decellularized non-COPD and COPD human lung ECM is not significantly different

Semi-quantitative mass spectrometry was used to initially assess differences in GAGs and other matrisomal proteins in native vs. decellularized lungs. We also were interested utilizing this approach for COPD as well as non-COPD lungs as work from our groups and others have shown differences in cellular growth on lung scaffolds and its ECM based on origin (e.g. species) and disease state, notably decreased growth and increased apoptosis of different lung cells cultured in decellularized human COPD lungs [5, 13, 24, 25]. Although some data exists analyzing the matrisome composition of native and decellularized lung tissue, diseased human tissue has not been studied in detail yet [1, 5, 8, 14–16, 24–33]. As we have previously observed for other classes of proteins [13], the matrisome composition of native and decellularized lungs varied only slightly with no significant differences observed in the number of individual proteins detected between different lungs including those from non-COPD and COPD patients (Appendix Figure 1). In detail, the overall detection of matrisome proteins (by number of individual proteins detected) was slightly increased in the decellularized lungs (native: 192 proteins for non-COPD patients, 187 for COPD; decellularized: 224 for non-COPD, 217 for COPD, Appendix Figure 1A). A relative proportional increase in secreted factors, glycoproteins, and proteoglycans was observed while ECM regulators and ECM affiliated proteins were proportionally decreased in the decellularized tissues. The relative percentage of collagens was comparable between native and decellularized non-COPD and COPD lungs. Proportionally a higher number of different glycoproteins, proteoglycans, and secreted factors were identified in the decellularized tissues as percent of total proteins detected. The percentage of matrisome-associated proteins as proportion of the total number of proteins identified was comparable around

90% for all four groups (native: 85.4±4.7% non-COPD, 87.0±2.5% COPD; decellularized: 89.5±0.8% non-COPD, 89.8±1.9% COPD). A detailed overview of the proteins identified is depicted in Appendix Figure 1B. We specifically did not find a notable difference in the number of proteoglycans detected in non-COPD and COPD lungs in native as well as decellularized tissue (Figure 1). The main proteoglycans found in the lung were comparably detected in both non-COPD and COPD tissues with only a few proteoglycans of unknown function in the lung differentially found in either native or decellularized non-COPD vs. COPD lungs.

Decellularization reduces the total amount of GAGs but differentially reduces specific GAG classes

Total lung GAG content is well recognized to decrease with decellularization as assessed predominantly in qualitative fashion by histologic staining with Alcian blue or general quantification of sulfated GAGs [13, 15, 34, 35]. Exploring this further with specific quantitative approaches for the major GAG classes HS, CS/DS, and HA demonstrated that decellularization significantly reduced total GAGs from 951 ± 608 ng/mg to 100 ± 89 ng/mg in lungs from non-smokers, from 1060 ± 437 ng/mg to 249 ± 186 ng/mg in lungs from ex-smokers, and from 1002 ± 455 ng/mg to 186 ± 79 ng/mg in lungs from COPD patients (Figure 2A). HS and CS/DS were significantly reduced, and although a trend was observed, decellularization did not lead to a statistically significant decrease in absolute HA content (Figure 2B–D). No statistically significant differences were observed comparing the total amount of GAGs, HS, CS/DS, or HA in native or decellularized tissue comparing non-smokers, ex-smokers, and COPD patients. Using PCA, a clear distinction of native vs. decellularized tissue was found reinforcing that the GAG content and composition is significantly impacted by the decellularization process (Figure 2E). These differences were predominantly seen in PC1, which accounted for 63.6 % of the statistical separation of the total variance between native and decellularized samples. No influence of smoking status, disease state, age, gender, and time to autopsy before tissue curation and subsequent decellularization was observed (Appendix Figure 2).

Immunohistochemical staining demonstrates qualitative absence of HS and CS/DS in decellularized lungs.

Previous histologic studies utilizing Alcian blue to assess total GAGs have not discriminated between different major GAG classes. Utilizing antibodies specific for HS or CS/DS, widespread distribution of immunostaining was observed throughout airways, vasculature, and parenchyma in representative native non-COPD and COPD lungs, as had previously been observed in a parallel study of GAGs in native normal and IPF lungs [9] (Figure 3). For HS the 10E4 antibody utilized recognizes HS epitopes with *N*-sulfated glucosamine residues and binds to a broad spectrum of HS polymers. In order to differentiate positive staining from background consecutive tissue sections were pretreated with a mixture of heparinase II and III that has been shown to degrade the epitope recognized by the antibody [9, 36]. In native tissue HS was mainly identified in basement membranes of small airways, blood vessels, and capillaries but also in smooth muscle cells in airways and blood vessels (Figure 3). There was however some residual background staining that was not abolished by the enzyme pretreatment. In decellularized tissue considerably less staining was observed

in similar overall distributions. Most of this was removed by the enzyme pretreatment but the background staining remained at similar levels. This suggests that the decellularization process removed a major part of HS present in native tissue. No significant qualitative differences were observed in non-COPD vs. COPD lungs although only a limited number of decellularized lungs have been analyzed to date.

For CS/DS the CS56 antibody utilized has been shown to recognize epitopes with 4 or 6-sulfated GalNAc followed by glucuronic acid residues but not iduronic acid [37]. Relative presence of iduronic acid is important for binding of matrix-associated growth factors such as HGF to its receptor c-MET as the binding affinity increases with increasing sulfate density of the GAG chains with higher amounts of iduronic acid, i.e., DS and HS rather than CS [49]. However, it cannot be excluded that the antibody can also bind to dermatan sulfate as iduronic acid residues can be interspersed between stretches of disaccharides with glucuronic acid. In native tissue, CS56-bound epitopes were located in basement membranes of small airways and blood vessels of varying size, in small airway epithelium, and in the submucosa of small airways and blood vessels (Figure 3). Pretreatment with chondroitinase ABC, which degrades these epitopes abolished most staining with only a small amount of residual background staining remaining. In decellularized tissue there was only minimal staining that was similarly removed by the enzyme pretreatment leaving similar levels of residual background staining. No significant qualitative differences were observed in non-COPD vs. COPD lungs although, as with HS staining, only a limited number of decellularized lungs have been analyzed to date. These results along with those observed for HS staining support the quantitative data (Figure 2) showing that the majority of HS and of CS/DS is lost during the decellularization process and that there are no significant differences in loss of GAGs between non-COPD and COPD lungs.

Decellularization differentially alters the disaccharide composition of HS and CS/DS in non-COPD and COPD lungs

Matrix-associated growth factor binding to and activation by GAGs is dependent on the GAG side chains and sulfation patterns. However, there is no available information on effects of decellularization on specific GAG side chains, including any potential differences between non-diseased (non-COPD) vs. diseased COPD lungs. We found that decellularization differentially reduced the amount of HS and CS/DS with specific side chains with the same trend in all three groups analyzed (non-smoker, ex-smoker, COPD) (Figure 4A, Appendix Figure 3). In detail, for HS, this involved significant reduction of the non-sulfated disaccharide UA-GlcNAc (0S) for ex-smokers and COPD patients, a significant reduction the of 6-sulfated disaccharide UA-GlcNAc-6S (6S) for COPD patients, and a significant reduction the *N*-sulfated disaccharides UA-GlcNS (NS) and UA-2S-GlcNS (NS2S) and in CS/DS the 4-sulfated disaccharide UA-GalNAc-4S (4S) CS/DS for all patient groups. This resulted in a significant relative increase in the *N*-sulfated disaccharide UA-GlcNS (NS) in HS for all patient groups, a significant relative increase in UA-GlcNAc (0S) for non-smokers and ex-smokers, and a significant relative decrease of UA-2S-GlcNS (NS2S) for ex-smokers (Appendix Figure 3). For CS/DS, the relative amounts of the disaccharides UA-GalNAc (0S) and UA-GalNAc-6S (6S) were significantly increased for non-smokers and ex-smokers while UA-GalNAc-4S (4S) was significantly

decreased in all patient groups (Appendix Figure 3). No significant difference in specific sulfation composition was observed between non-smokers, ex-smokers, and COPD patients. PCA showed a clear distinction of native vs. decellularized tissue for the specific GAG composition (HS, CS/DS) (Figure 4B). These differences were predominantly seen in PC1 for both HS and CS/DS, which accounted for 48.3 % (HS) and 54.3 % (CS/DS) of the statistical separation of the total variance between native and decellularized samples. No influence of smoking status, disease state, age, gender, and time to autopsy before tissue curation and decellularization was observed (Appendix Figure 4).

Decellularization abolishes matrix-associated growth factor binding by GAGs isolated from decellularized non-COPD human lung ECM

As specific GAGs were decreased and/or proportionally changed following decellularization, it is important to further determine whether function of the GAGs remaining in the decellularized lungs has been altered, specifically ability of the remaining GAGs to bind matrix-associated growth factors. Using surface plasmon resonance, HS and CS/DS isolated from native non-COPD lung ECM homogenates were found to be capable of binding FGF2, HGF, and TGFβ1 (Figure 5). In general HS exhibited a slightly higher binding affinity than CS. Binding affinity to HGF was higher than for FGF2 and TGFβ1. In contrast, none of these matrix-associated growth factors were able to bind to HS or CS/DS isolated from decellularized non-COPD lung ECM homogenates (Figure 5). These results demonstrate that in addition to depletion of and/or proportionate change in total GAGs, specific GAG classes, and/or specific side chains, the GAGs remaining in decellularized non-COPD (non-COPD) human lungs were dysfunctional. Concentration-dependent binding kinetics of the matrix-associated growth factors to native tissue are depicted in Appendix Figure 5 and Appendix Table 2. No binding of growth factors to HS or CS/DS isolated from decellularized non-COPD lung ECM homogenates was detected at any of the concentrations tested (data not shown).

Combinatorial replenishment of HS, CS, or DS with and without matrix-associated growth factors significantly effects growth of lung cells in standard tissue culture

As HS, CS, and DS are depleted in decellularized lungs and further unable to bind TGFβ1, HGF, or FGF2, we hypothesized that it might be necessary to replenish these GAGs and/or matrix-associated growth factors to optimize cell growth during recellularization. To initially evaluate this, the dose- (0.001 – 10 μM) and time- (1–5 days) dependent effects of HS, CS, or DS on growth of representative differentiated lung cells, including human bronchial epithelial cells (HBE), human pulmonary vascular endothelial cells (CBF), and human lung fibroblasts (HLF), were initially assessed utilizing cells plated on the surface of standard tissue culture wells (Appendix Figure 6). Using metabolic activity, as assessed with the Alamar Blue assay, as a surrogate for cell growth, overall there was no significant difference in metabolic activity of CBF cells at the different concentrations and time points. The metabolic activity of HBE cells was comparable at lower GAG concentrations but higher concentrations of 5 and 10 μM led to a reduction in activity with each of the different GAGs added. HLF cells exhibited differential effects depending on time point and GAG added from which no clear conclusion could be drawn. In general, a higher concentration of 5–10

μM seemed to increase metabolic activity in those cells on day 3 but this effect was gone on day 5.

This model system was also utilized to analyze the effect of the matrix-associated growth factors, FGF2, HGF, TGFβ1 added at representative relevant concentrations in combination with GAGs to the cultivation medium. A single representative concentration of 1 μM was chosen for the GAGs as the highest concentration that did not positively or negatively influence cell metabolic activity (Appendix Figure 6). A concentration of 5 μM was utilized in the 3D cell culture model since it is in the biologically relevant range in native tissue. In the 2D studies, assessing effects of soluble GAGs, concentrations of 5 and 10 μM decreased cell viability and we therefore used a lower concentration of 1 μM (Appendix Figure 6). As with addition of the GAGs alone, addition of growth factors had differential time- and combination-dependent effects on metabolic activity of the different cell types (day 5 time point depicted in Figure 6A, day 3 depicted in Appendix Figure 7). The data presented in Figure 6A represents metabolic activity of the combination treatments normalized to the respective GAG without addition of growth factor. Parallel data normalized to the respective growth factor without addition of GAG is shown in Appendix Figure 7.

Notably, the combination of HS and CSA with FGF2 significantly reduced metabolic activity of CBF cells. Addition of FGF2 alone and in combination with either HS or CSA increased HBE metabolic activity at all time points (Figure 6A). In contrast, addition HGF resulted in decreased metabolic activity independent of its administration alone or in combination with any of the GAGs. Similarily the addition of TGFβ1 in combination with HS and CSA resulted in decreased metabolic activity in HBE cells. HLFs showed reduced metabolic activity with the addition of TGFβ1 alone, when FGF2 was added in combination CSA and DS and for HGF in combination with the addition of DS.

Replenishment of HS, CS, or DS into type I collagen gels significantly effects growth of lung cells in a dose and time-dependent manner

The above tissue culture studies demonstrated that combinatorial addition of soluble GAGs and matrix-associated growth factors had significant yet differential effects on growth of the representative lung cell types as recognized in the previous studies [27]. As GAGs are generally bound to their core proteins in the ECM, it was important to next examine their effects under a more relevant physiologic condition, notably combinatorial effects on cell growth of GAGs incorporated into decellularized human lung ECM gels coated with different matrix-associated growth factors. To evaluate this, GAGs at different concentrations from a low range (0.1 μM) to more biologically relevant concentrations (1 and 5 μM) were initially incorporated into type I collagen gels. As depicted in Appendix Figure 8, the observed effects differed depending on cell type, GAG type, GAG concentration, and days in culture. For CBFs, a significant dose-dependent increase in metabolic activity was observed with CSA in general, with HS on day 3, and with DS on day 7. HLFs demonstrated a significant dose-dependent increase in metabolic activity with DS in general and with CSA and HS on day 7. HBEs did not demonstrate a significant dose-dependent change in metabolic activity. When comparing the addition of different GAGs, DS led to a significant increase in metabolic activity of HLF cells compared to HS

and CSA especially at a concentration of 5 μM and at the later time points. In CBFs, a decrease in metabolic activity with DS in comparison to HS and CSA was observed only on day 3 and only for a concentration of 5 μM in contrast to results observed when the GAGs were added in solution where no significant difference was observed (Figure 6A). Besides the significant increase in metabolic activity in HBE cells on day 7 with 5 μM DS in comparison to HS and CSA, no other significant effects were observed. Overall the results with the CBFs and HLFs were more consistent over repeat experiments and had less variation in comparison to the results observed with the HBEs.

Combinatorial replenishment of HS, CS, or DS with and without matrix-associated growth factors significantly affects metabolic activity of lung cells cultured in or on hybrid decellularized human lung ECM/type I collagen ECM gels.

The combinatorial effects on cell metabolic activity of GAGs incorporated into decellularized human lung ECM gels with or without addition of representative matrix-associated growth factors was next evaluated. As the mechanical properties of the ECM gels might differ with materials from different individual decellularized human lungs, the ECM gels were reinforced with type 1 collagen to create a hybrid decellularized human lung ECM/type I collagen gel. GAGs were incorporated at a representative biologically relevant concentration (5 μM) into the gels, incubated overnight with the different matrix-associated growth factor solutions to achieve coating, and cells subsequently seeded onto the matrix-associated growth factor-coated gel. No significant difference had previously been observed between individual decellularized human lung ECM gels obtained from either non-COPD (non-smoker/ex-smoker) or COPD patients (data not shown) and therefore the experiments were conducted with decellularized ECM from one representative non-COPD lung. The data presented in Figures 6B and 6C represents metabolic activity of the combination treatments normalized to the respective GAG without addition of growth factor. Parallel data normalized to the respective growth factor without addition of GAG is shown in Appendix Figures 10 and 11.

Addition of HS and CSA reduced metabolic activity of CBF cells when they were grown on top of type I collagen gels and when incorporated into human lung ECM/type 1 collagen gels. HBE cells showed a reduction in metabolic activity when DS was added to the human lung ECM/type I collagen gels and cells were grown on top. When HBE cells were incorporated into type 1 collagen gels in combination with any of the GAGs their metabolic activity was reduced. HLF cells had reduced metabolic activity when CSA was added to either of the gels and cells were grown on top but not when incorporated (Figures 6B and 6C).

Coating of the different matrix-associated growth factors onto type I collagen gels affected the different cell types in relatively comparable ways (Figures 6B and 6C). Overall, coating with TGFβ1 generally led to a decrease in metabolic activity independent of the GAG incorporated and the duration of culture time. Metabolic activity of the cells on TGFβ1 coated gels was consistently lower than for the coating of HGF and FGF onto the gels (data for the 5 day time points are depicted in Figures 6B and 6C, data for earlier and later time points are depicted in Appendix Figure 9).

Addition of the matrix-associated growth factors into gels resulted in generally comparable effects for both hybrid decellularized human lung ECM/type I collagen gels and the type I collagen control gels. In particular, reduced overall metabolic activity was observed with addition of TGFβ1 independent of GAG, cell type, or culture duration. However, addition of either FGF2 or HGF, either to type I collagen control gels alone or in combination with each GAG, promoted more notable relative metabolic activity especially for HBE cells (Figure 6, Appendix Figure 9). The largest effect was seen by combination of FGF2 with DS or CSA. A summary of the differential effects of GAG and/or growth factor addition is shown in Tables 3 and 4.

Representative low and high power magnification fluorescent images taken at the end of these studies capture colonization patterns and phenotype of the CBF, HBE, and HLF cells grown on type I collagen or decellularized human lung ECM/type I collagen gels with or without encapsulated GAGs and/or coated growth factors (Appendix Figure 12). HBE cells grown on either type I collagen or decellularized human lung ECM/type I collagen gels generally formed compact discrete colonies that tended to be equally distributed across the gels. Qualitatively denser colony formation was observed with addition of either HS or CSA. HLF cells tended to grow robustly across all the different gels with no obvious qualitative difference in growth patterns regardless of gel type, added GAG, or matrix-associated growth factor coating.

Discussion

Decellularized lungs and materials derived from them are increasingly utilized in lung regenerative medicine and engineering applications. However, there is growing evidence that the ECM, ECM-associated proteins, and other substances remaining after decellularization may be more fundamentally altered than previously appreciated and not capable of sustaining diverse and long-term cell growth [2, 38–40]. This may particularly be the case following detergent-based decellularization protocols in which the detergent utilized can potentially denature or otherwise degrade different ECM components and/or activate destructive enzymes such as matrix metalloproteinases [47]. While total GAGs have long been recognized to decrease after decellularization, detailed assessment of individual GAG depletion and potential functional effects have not yet been extensively addressed [41, 42]. Individual GAG depletion is important to ascertain as ECM proteoglycans and their GAG chains play critical roles in cellular growth, differentiation, and function [7, 10]. Understanding the effects of the decellularization procedure on the GAG composition of the retained ECM and its capability to bind and retain matrix associated growth factors and added GAGs will be important for the interpretation of results generated from decellularized lung-derived materials such as (hydro-) gels and bioinks as well as for the recellularization of intact scaffolds. It is of further interest to evaluate this in diseased lungs wherein it is known that the remaining scaffold in decellularized COPD as well as IPF lungs differently affects behavior of inoculated cells compared to decellularized non-COPD lung matrices [13] but the reason for those effects still needs to be deciphered.

We therefore assessed human lungs obtained from autopsy for effects of a commonly utilized detergent-based decellularization protocol on content and function of major GAGs

and GAG chains remaining in the decellularized lungs. Initial focus for this study was in lungs from patients with either no significant discernible lung disease (non-COPD) or from those with COPD. The lungs utilized tended to be from older individuals as reflective of the demographics of lungs available through the University of Vermont autopsy service. Classification of the lungs into populations of non-COPD (non-smoker or ex-smoker with no diagnosed lung disease) or COPD (with or without active smoking at time of death) was based on available clinical information. We acknowledge this is an imperfect categorization and larger scale studies with larger numbers of lungs and more rigorous clinical classifications will be necessary to confirm and further explore the observed results.

Acknowledging these caveats, the current study provides new hypothesis-generating information on content, composition, and function of major GAG groups following decellularization of non-COPD and COPD lungs. Notably HS, CS, and DS are depleted while HA is proportionally increased compared to these other GAGs following decellularization. This was not a surprising finding as much of the total lung GAG content is cell-associated and therefore will be accordingly depleted upon cell removal. No significant difference was observed in the depletion of GAGs in decellularized scaffolds from different disease status (COPD vs. non-COPD) and smoking status (non-smoker vs. ex-smoker). These findings are paralleled by no overall significant difference in matrisomal proteins, particularly proteoglycans, between non-COPD and COPD lungs, as we had previously observed with other proteins groups retained in decellularized non-COPD vs. COPD lungs [16]. We acknowledge that the mass spectrometry techniques utilized result in semi-quantitative information and that other techniques can result in more quantitative data that could potentially show significant differences in specific proteins or protein groups [31]. In addition, low abundance proteins can be missed although these are generally more detectable following decellularization which likely accounts for the higher number of matrisomal proteins detected in decellularized vs. native tissues. Little is otherwise known about GAG composition of COPD lungs although parallel studies from our group suggest alterations in both HS and in CS/DS in different stages of COPD (Hallgren et al, unpublished data).

The disproportionate changes in specific GAG side chains following decellularization is a previously unknown observation that has potential functional ramifications as the different side chains have different roles in binding matrix-associated growth factors. For instance, binding of members of FGF ligand family to their receptors, including FGF1 and FGF2 to FGFR1 and FGFR2, has previously been shown to require *N*-, 2-*O*, and 6-*O* sulfated HS [43, 44]. In our experiments we did not observe this dependency based on the finding that the metabolic activity of HBEs was increased by FGF not only in the presence of HS but also CS and DS in human lung ECM/type I collagen gels. The bioactivity of TGFβ1 has also been demonstrated to be dependent on the degree of sulfation of HS polymers but it is not known if this interaction is specific or rather a matter of non-specific electrostatic interactions [45]. In accordance with TGFβ1, the binding of HGF to its receptor c-MET is dependent on electrostatic interactions with GAGs, as the binding affinity increase with increasing sulfate density of the GAG chains [46]. However, it has also been suggested that this interaction is favored by GAGs with higher amounts of iduronic acid i.e. DS and HS rather than CS. Analysis of the iduronic content of the GAGs utilized in the cell culture experiments demonstrated low amounts in CSA but about 20% in HS and 85%

in DS (**Appendix Table 4**). However, HGF significantly increased the metabolic activity of HBE cells in the presence of CS and DS but not HS, suggesting that the iduronic acid content played a minor role in the type I collagen and the mixed decellularized human lung ECM/type I collagen gel culture systems. HGF is also specifically important to epithelial spreading and phenotypic maintenance and thus may be particularly germane to lung regeneration efforts [47, 48].

Qualitative assessments of specific HS and CS/DS localization via immunostaining before and after decellularization demonstrated that, as previously observed, these GAGs are widespread throughout native lung, presumably much of which is cell-associated [9]. Both HS and CS/DS appeared to be qualitatively decreased after decellularization, which correlates with the quantitative data demonstrating decrease in each GAG following decellularization. However, at present it is not clear if the residual staining reflects actual HS or CS/DS staining or rather nonspecific antibody staining to debris. Intriguingly, it raises the possibility that epitopes, recognized by the antibodies, have been altered in the decellularization process. No obvious differences were observed between non-COPD and COPD lungs although we acknowledge that only a small number of lungs were assessed. A broader evaluation of an increased number of lungs across the spectrum of COPD will need to be done prior to making any more detailed analyses.

Notably, HS, CS, and DS isolated from decellularized human lungs are no longer able to bind key matrix-associated growth factors FGF2, HGF, or TGFβ1. Whether this reflects loss of specific side chains and corresponding matrix-associated growth factor binding capacities remains to be determined. Nonetheless, this is a heretofore-unrecognized aspect of lung decellularization that has significant potential ramifications on growth and function of cells inoculated into decellularized scaffolds or materials derived from them. FGF2 is critically involved in lung development and repair and the most abundant FGF in the lung [49]. TGFβ1 has critical roles in cell growth and differentiation as well as in the regulation of lung inflammatory processes. HGF plays a role in lung development, inflammation, repair, and regeneration and has recently been discussed as potential treatment target for pulmonary fibrosis [50]. As such, inability of decellularized scaffolds or derivative materials to properly utilize any of these matrix-associated growth factors may have significant deleterious effects on cell growth and differentiation during recellularization. Some limited recent data suggest that HS is critical for supporting growth and differentiation of lung progenitor cells seeded into decellularized rat lung ECM scaffolds [3]. However, it is unclear whether this is a direct effect of HS or of matrix-associated growth factors binding to HS. A related study demonstrated increased proliferation and decreased senescence of basal epithelial stem cells (BESCs) isolated from adult human lung tissue when cultivated on collagen IV-coated tissue culture plates supplemented with two other glycoproteins (Fibrillin 2 and Tenascin C) [5] showing the importance of GAGs in recellularization schemes. However, here as well, the role of matrix-associated growth factor interaction with the glycoproteins had not yet been elucidated.

To further explore this, we assessed effects of combinatorial addition of HS, CS, or DS with FGF2, HGF, or TGFβ1 on growth of a spectrum of representative lung cells using gels derived from the decellularized lungs as a model system. Initial proof of concept

studies with addition of either GAG or matrix-associated growth factor in soluble form to routine tissue culture plates demonstrated differential effects on cell growth by type and concentration of GAG, specific matrix-associated growth factor, and duration of cell culture. Subsequently using two gel models, type 1 collagen and hybrid decellularized human lung ECM/type 1 collagen, in which the different lung cells were cultured either on top of or embedded within the gels, demonstrated differential effects of the type of gel, type and concentration of GAG, matrix-associated growth factor addition, and duration of culture on cell metabolic activity. Overall, there was often a more robust effect by the combination of GAGs with matrix-associated growth factors compared to either GAGs or matrix-associated growth factors alone although this differed with the cell type. This suggests both matrix-associated growth factor-dependent and –independent GAG effects and in parallel GAG-dependent and –independent matrix-associated growth factor effects.

Further, differences in GAG/matrix-associated growth factors between cells-on-gels vs. cells-in-gels suggest that orientation of the GAGs and growth factors can modulate the magnitude of the effect on cell growth. The morphology of HBE and CBF cells grown within type I collagen and decellularized human lung ECM/type I collagen hybrid gels was significantly altered in comparison to their counterparts grown on top of the gels. CBFs were able to proliferate and colonize gel conditions when grown on the surface, often organizing into tube-like networks. CBFs encapsulated within type I collagen or decellularized human lung ECM/type I collagen gels remain viable and proliferate slowly, however they did not demonstrate the same colonizing or self-organizing potential within the 3D cultures. Unlike CBFs, both the HBE and HLF cell lines showed similar proliferative potential when comparing cells grown on the surface to those encapsulated within the gels. However, HBEs were found to have differential morphology in the two culture systems. On the surface of type I collagen or decellularized human lung ECM/type I collagen gels, the HBEs spread out and mostly adopted a mono-layer like epithelial phenotype. However, when encapsulated within the gels they self-organized into loose clusters. While they did not form complete spheroids within the short time scale studied, the behavior suggests that the 3D culture format of cells within gels increases cell-cell interactions when compared to the 2D format of cells grown on top of gels. Overall, as the cells encapsulated within the 3D gels were more thoroughly exposed to the GAGs and growth factors this may explain the increased effect observed in case of the CBF and HLFs cells, as compared to more limited interaction of cells on top of the gel surfaces.

It is important to reinforce that the results obtained are specific for the decellularization protocol utilized. Other protocols with different detergents or physical methods such as freeze-thawing may yield different results. Different concentrations of or incubation times with the same detergents utilized, TritonX-100, and sodium deoxycholate, might also result in different results. As GAG content and sulfation patterns are increasingly recognized to change with age and disease [51, 52], future studies will also explore further variables such as age and other diseases, particularly IPF. We further acknowledge that only a single concentration of growth factors was investigated and different concentration-dependent results may otherwise be observed. Additionally, GAGs contribute to local lung viscoelastic behavior, for regulation of water diffusion, and water stabilization properties of GAGs in the interstitial spaces are critical for normal barrier function and prevention of edema. These

will be critical aspects to further assess as techniques are developed to effectively replenish GAGs in decellularized lungs in order to optimize recellularization schemes. However, this will need to be further balanced against potential production of GAGs and matrix-associated growth factors by the cells seeded into decellularized whole lungs or into gels or bioinks produced from the decellularized lungs. We are currently investigating this as well as GAG-matrix associated growth factor interactions in other systems including precision cut lung slices.

Conclusion

Our results demonstrate that specific GAG types and/or the GAG disaccharide composition are lost during a commonly utilized detergent-based decellularization process. Decellularized lungs and gels derived from them are significantly impaired in their ability to bind critical matrix-associated growth factors and to support cell metabolism. Systematically adding back selected GAGs and matrix-associated growth factors has differential effects on growth of representative lung epithelial, stromal, and pulmonary vascular endothelial cells in several model culture systems including one utilizing decellularized human lung ECM as a culture substrate. Future studies will probe in more detail the relationship of each GAG type, side chains, and matrix-associated growth factor on growth of lung cells in gel models derived from both normal and abnormal decellularized human lungs and use to develop informed schemes for enhancing recellularization of intact decellularized whole lung scaffolds.

Supplementary Material

Refer to Web version on PubMed Central for supplementary material.

Acknowledgements

The authors thank Jacob Dearborn, Nathan Gasek, Aniruddha Bhattacharyya, Amy Coffey, Amelia Payne, Sean Wrenn, Ethan Griswold, Robert Hommel, Tovah Moss, Benefsha Mohammad, and Jessica Louie for help with the decellularization of the lung tissue. Thanks to Mervin Yoder for providing the CBF cells and Catrina Hood, Bethany Ahlers, Bin Deng, and Ying Wai Lam from the Vermont Genetics Network for help with the Mass spectrometry. The image of the human torso in the graphical abstract was taken from Biorender.com.

This work was supported by the National Institutes of Health, RO1 HL12714401, 2014 (DJW); NHBLI Lung Biology Training grant T32 HL076122, 2016 (RAP); DK111958, 2017 (RJL); CA231074, 2018 (RJL); HL125371, 2016 (RJL); NS088496, 2016 (RJL); Marie Curie Post-doctoral Research Fellowship (RESPIRE3) from the European Respiratory Society and the European Union's H2020 research and innovation programme 713406, 2018 (SRE); Swedish Research Council in Medicine and Health 11550 (GWT); Swedish Heart-Lung Foundation (GWT); Royal Physiographical Society in Lund (GWT); Medical Faculty of Lund University (GWT); Gustaf V's och Drottning Victorias Frimurare Foundation (GWT); the Consul Thure Carlsson Foundation, ALF Grants Region Skåne and the Swedish Foundation for Strategic Research (GWT); King Gustav V's and Queen Victoria's Freemason Foundation (OH).

References

[1]. Balestrini JL, Gard AL, Gerhold KA, Wilcox EC, Liu A, Schwan J, Le AV, Baevova P, Dimitrievska S, Zhao L, Sundaram S, Sun H, Rittie L, Dyal R, Broekelmann TJ, Mecham RP, Schwartz MA, Niklason LE, White ES, Comparative biology of decellularized lung matrix: Implications of species mismatch in regenerative medicine, Biomaterials 102 (2016) 220–30. [PubMed: 27344365]

[2]. Daly AB, Wallis JM, Borg ZD, Bonvillain RW, Deng B, Ballif BA, Jaworski DM, Allen GB, Weiss DJ, Initial binding and recellularization of decellularized mouse lung scaffolds with bone marrow-derived mesenchymal stromal cells, Tissue Eng Part A 18(1–2) (2012) 1–16. [PubMed: 21756220]

[3]. Lecht S, Stabler CT, Rylander AL, Chiaverelli R, Schulman ES, Marcinkiewicz C, Lelkes PI, Enhanced reseeding of decellularized rodent lungs with mouse embryonic stem cells, Biomaterials 35(10) (2014) 3252–62. [PubMed: 24439414]

[4]. Linhardt RJ, Toida T, Role of glycosaminoglycans in cellular communication, Acc Chem Res 37(7) (2004) 431–8. [PubMed: 15260505]

[5]. Gilpin SE, Li Q, Evangelista-Leite D, Ren X, Reinhardt DP, Frey BL, Ott HC, Fibrillin-2 and Tenascin-C bridge the age gap in lung epithelial regeneration, Biomaterials 140 (2017) 212–219. [PubMed: 28662401]

[6]. Godin LM, Sandri BJ, Wagner DE, Meyer CM, Price AP, Akinnola I, Weiss DJ, Panoskaltsis-Mortari A, Decreased Laminin Expression by Human Lung Epithelial Cells and Fibroblasts Cultured in Acellular Lung Scaffolds from Aged Mice, PLoS One 11(3) (2016) e0150966.

[7]. Soares da Costa D, Reis RL, Pashkuleva I, Sulfation of Glycosaminoglycans and Its Implications in Human Health and Disorders, Annu Rev Biomed Eng 19 (2017) 1–26. [PubMed: 28226217]

[8]. Burgstaller G, Oehrle B, Gerckens M, White ES, Schiller HB, Eickelberg O, The instructive extracellular matrix of the lung: basic composition and alterations in chronic lung disease, Eur Respir J 50(1) (2017).

[9]. Westergren-Thorsson G, Hedstrom U, Nybom A, Tykesson E, Ahrman E, Hornfelt M, Maccarana M, van Kuppevelt TH, Dellgren G, Wildt M, Zhou XH, Eriksson L, Bjermer L, Hallgren O, Increased deposition of glycosaminoglycans and altered structure of heparan sulfate in idiopathic pulmonary fibrosis, Int J Biochem Cell Biol 83 (2017) 27–38. [PubMed: 27974233]

[10]. Schultz V, Suflita M, Liu X, Zhang X, Yu Y, Li L, Green DE, Xu Y, Zhang F, DeAngelis PL, Liu J, Linhardt RJ, Heparan Sulfate Domains Required for Fibroblast Growth Factor 1 and 2 Signaling through Fibroblast Growth Factor Receptor 1c, J Biol Chem 292(6) (2017) 2495–2509. [PubMed: 28031461]

[11]. Sterner E, Masuko S, Li G, Li L, Green DE, Otto NJ, Xu Y, DeAngelis PL, Liu J, Dordick JS, Linhardt RJ, Fibroblast growth factor-based signaling through synthetic heparan sulfate blocks copolymers studied using high cell density three-dimensional cell printing, J Biol Chem 289(14) (2014) 9754–65. [PubMed: 24563485]

[12]. Sterner E, Meli L, Kwon SJ, Dordick JS, Linhardt RJ, FGF-FGFR signaling mediated through glycosaminoglycans in microtiter plate and cell-based microarray platforms, Biochemistry 52(50) (2013) 9009–19. [PubMed: 24289246]

[13]. Wagner DE, Bonenfant NR, Parsons CS, Sokocevic D, Brooks EM, Borg ZD, Lathrop MJ, Wallis JD, Daly AB, Lam YW, Deng B, DeSarno MJ, Ashikaga T, Loi R, Weiss DJ, Comparative decellularization and recellularization of normal versus emphysematous human lungs, Biomaterials 35(10) (2014) 3281–97. [PubMed: 24461327]

[14]. DE F.W. Uhl; Weiss DJ, Preparation of Decellularized Lung Matrices for Cell Culture and Protein Analysis in Fibrosis: Methods and Protocols, Methods in Molecular Biology, Springer Science+Business Media LLC 1627 (2017) 253–283.

[15]. Wagner DE, Bonenfant NR, Sokocevic D, DeSarno MJ, Borg ZD, Parsons CS, Brooks EM, Platz JJ, Khalpey ZI, Hoganson DM, Deng B, Lam YW, Oldinski RA, Ashikaga T, Weiss DJ, Three-dimensional scaffolds of acellular human and porcine lungs for high throughput studies of lung disease and regeneration, Biomaterials 35(9) (2014) 2664–79. [PubMed: 24411675]

[16]. Platz J, Bonenfant NR, Uhl FE, Coffey A, McKnight T, Parsons C, Sokocevic D, Borg ZD, Lam YW, Deng B, Fields J, Desarno M, Loi R, Hoffman A, Bianchi J, Dacken B, Petersen T, Wagner DE, Weiss DJ, Comparative study to the use of decellularized alpha-Gal KO pig lungs for xenogeneic lung transplantation, Tissue Eng Part C Methods (2016).

[17]. Naba A, Clauser KR, Hoersch S, Liu H, Carr SA, Hynes RO, The matrisome: in silico definition and in vivo characterization by proteomics of normal and tumor extracellular matrices, Mol Cell Proteomics 11(4) (2012) M111 014647.

[18]. Noborn F, Gomez Toledo A, Sihlbom C, Lengqvist J, Fries E, Kjellen L, Nilsson J, Larson G, Identification of chondroitin sulfate linkage region glycopeptides reveals prohormones as a novel class of proteoglycans, Mol Cell Proteomics 14(1) (2015) 41–9. [PubMed: 25326458]

[19]. Lindahl U, Couchman J, Kimata K, Esko JD, Proteoglycans and Sulfated Glycosaminoglycans, in: rd A.Varki, Cummings RD, Esko JD, Stanley P, Hart GW, Aebi M, Darvill AG, Kinoshita T, Packer NH, Prestegard JH, Schnaar RL, Seeberger PH (Eds.), Essentials of Glycobiology, Cold Spring Harbor (NY), 2015, pp. 207–221.

[20]. Volpi N, Galeotti F, Yang B, Linhardt RJ, Analysis of glycosaminoglycan-derived, precolumn, 2-aminoacridone-labeled disaccharides with LC-fluorescence and LC-MS detection, Nat Protoc 9(3) (2014) 541–58. [PubMed: 24504479]

[21]. Li G, Li L, Tian F, Zhang L, Xue C, Linhardt RJ, Glycosaminoglycanomics of cultured cells using a rapid and sensitive LC-MS/MS approach, ACS Chem Biol 10(5) (2015) 1303–10. [PubMed: 25680304]

[22]. Zhang F, Lee KB, Linhardt RJ, SPR Biosensor Probing the Interactions between TIMP-3 and Heparin/GAGs, Biosensors (Basel) 5(3) (2015) 500–12. [PubMed: 26213979]

[23]. Hetzel M, Bachem M, Anders D, Trischler G, Faehling M, Different effects of growth factors on proliferation and matrix production of normal and fibrotic human lung fibroblasts, Lung 183(4) (2005) 225–37. [PubMed: 16211459]

[24]. Sokocevic D, Bonenfant NR, Wagner DE, Borg ZD, Lathrop MJ, Lam YW, Deng B, Desarno MJ, Ashikaga T, Loi R, Hoffman AM, Weiss DJ, The effect of age and emphysematous and fibrotic injury on the re-cellularization of de-cellularized lungs, Biomaterials 34(13) (2013) 3256–69. [PubMed: 23384794]

[25]. Booth AJ, Hadley R, Cornett AM, Dreffs AA, Matthes SA, Tsui JL, Weiss K, Horowitz JC, Fiore VF, Barker TH, Moore BB, Martinez FJ, Niklason LE, White ES, Acellular normal and fibrotic human lung matrices as a culture system for in vitro investigation, Am J Respir Crit Care Med 186(9) (2012) 866–76. [PubMed: 22936357]

[26]. Schiller HB, Fernandez IE, Burgstaller G, Schaab C, Scheltema RA, Schwarzmayr T, Strom TM, Eickelberg O, Mann M, Time- and compartment-resolved proteome profiling of the extracellular niche in lung injury and repair, Mol Syst Biol 11(7) (2015) 819. [PubMed: 26174933]

[27]. Calle EA, Hill RC, Leiby KL, Le AV, Gard AL, Madri JA, Hansen KC, Niklason LE, Targeted proteomics effectively quantifies differences between native lung and detergent-decellularized lung extracellular matrices, Acta Biomater 46 (2016) 91–100. [PubMed: 27693690]

[28]. Hill RC, Calle EA, Dzieciatkowska M, Niklason LE, Hansen KC, Quantification of extracellular matrix proteins from a rat lung scaffold to provide a molecular readout for tissue engineering, Mol Cell Proteomics 14(4) (2015) 961–73. [PubMed: 25660013]

[29]. Li Q, Uygun BE, Geerts S, Ozer S, Scalf M, Gilpin SE, Ott HC, Yarmush ML, Smith LM, Welham NV, Frey BL, Proteomic analysis of naturally-sourced biological scaffolds, Biomaterials 75 (2016) 37–46. [PubMed: 26476196]

[30]. Gilpin SE, Guyette JP, Ren X, Gonzalez G, Xiong L, Song JJ, Vacanti J, Ott HC, Up-Scaling Decellularization and Whole Organ Culture for Human Lung Regeneration, Journal of Heart and Lung Transplantation 32(4) (2013) S69–S70.

[31]. Charest JM, Okamoto T, Kitano K, Yasuda A, Gilpin SE, Mathisen DJ, Ott HC, Design and validation of a clinical-scale bioreactor for long-term isolated lung culture, Biomaterials 52 (2015) 79–87. [PubMed: 25818415]

[32]. Guyette JP, Gilpin SE, Charest JM, Tapias LF, Ren X, Ott HC, Perfusion decellularization of whole organs, Nat Protoc 9(6) (2014) 1451–68. [PubMed: 24874812]

[33]. Petersen TH, Calle EA, Colehour MB, Niklason LE, Matrix Composition and Mechanics of Decellularized Lung Scaffolds, Cells Tissues Organs 195(3) (2011) 222–31. [PubMed: 21502745]

[34]. Gilpin SE, Guyette JP, Gonzalez G, Ren X, Asara JM, Mathisen DJ, Vacanti JP, Ott HC, Perfusion decellularization of human and porcine lungs: bringing the matrix to clinical scale, J Heart Lung Transplant 33(3) (2014) 298–308. [PubMed: 24365767]

[35]. Ott HC, Clippinger B, Conrad C, Schuetz C, Pomerantseva I, Ikonomou L, Kotton D, Vacanti JP, Regeneration and orthotopic transplantation of a bioartificial lung, Nat Med 16(8) (2010) 927–33. [PubMed: 20628374]

[36]. van den Born J, Salmivirta K, Henttinen T, Ostman N, Ishimaru T, Miyaura S, Yoshida K, Salmivirta M, Novel heparan sulfate structures revealed by monoclonal antibodies, J Biol Chem 280(21) (2005) 20516–23. [PubMed: 15778504]

[37]. Ito Y, Hikino M, Yajima Y, Mikami T, Sirko S, von Holst A, Faissner A, Fukui S, Sugahara K, Structural characterization of the epitopes of the monoclonal antibodies 473HD, CS-56, and MO-225 specific for chondroitin sulfate D-type using the oligosaccharide library, Glycobiology 15(6) (2005) 593–603. [PubMed: 15625183]

[38]. Zhou Y, Horowitz JC, Naba A, Ambalavanan N, Atabai K, Balestrini J, Bitterman PB, Corley RA, Ding BS, Engler AJ, Hansen KC, Hagood JS, Kheradmand F, Lin QS, Neptune E, Niklason L, Ortiz LA, Parks WC, Tschumperlin DJ, White ES, Chapman HA, Thannickal VJ, Extracellular matrix in lung development, homeostasis and disease, Matrix Biol (2018).

[39]. Niklason LE, Understanding the Extracellular Matrix to Enhance Stem Cell-Based Tissue Regeneration, Cell Stem Cell 22(3) (2018) 302–305. [PubMed: 29499149]

[40]. Wallis JM, Borg ZD, Daly AB, Deng B, Ballif BA, Allen GB, Jaworski DM, Weiss DJ, Comparative assessment of detergent-based protocols for mouse lung de-cellularization and re-cellularization, Tissue Eng Part C Methods 18(6) (2012) 420–32. [PubMed: 22165818]

[41]. Shojaie S, Ermini L, Ackerley C, Wang J, Chin S, Yeganeh B, Bilodeau M, Sambi M, Rogers I, Rossant J, Bear Christine E., Post M, Acellular Lung Scaffolds Direct Differentiation of Endoderm to Functional Airway Epithelial Cells: Requirement of Matrix-Bound HS Proteoglycans, Stem Cell Reports 4(3) (2015) 419–430. [PubMed: 25660407]

[42]. Garlikova Z, Silva AC, Rabata A, Potesil D, Ihnatova I, Dumkova J, Koledova Z, Zdrahal Z, Vinarsky V, Hampl A, Pinto-do OP, Nascimento DS, Generation of a Close-to-Native In Vitro System to Study Lung Cells-Extracellular Matrix Crosstalk, Tissue Eng Part C Methods 24(1) (2018) 1–13. [PubMed: 28895470]

[43]. Settembre C, Arteaga-Solis E, McKee MD, de Pablo R, Al Awqati Q, Ballabio A, Karsenty G, Proteoglycan desulfation determines the efficiency of chondrocyte autophagy and the extent of FGF signaling during endochondral ossification, Genes Dev 22(19) (2008) 2645–50. [PubMed: 18832069]

[44]. Powell AK, Fernig DG, Turnbull JE, Fibroblast growth factor receptors 1 and 2 interact differently with heparin/heparan sulfate. Implications for dynamic assembly of a ternary signaling complex, J Biol Chem 277(32) (2002) 28554–63. [PubMed: 12034712]

[45]. Koehler L, Samsonov S, Rother S, Vogel S, Kohling S, Moeller S, Schnabelrauch M, Rademann J, Hempel U, Pisabarro MT, Scharnweber D, Hintze V, Sulfated Hyaluronan Derivatives Modulate TGF-beta1:Receptor Complex Formation: Possible Consequences forTGF-beta1 Signaling, Sci Rep 7(1) (2017) 1210. [PubMed: 28446792]

[46]. Catlow KR, Deakin JA, Wei Z, Delehedde M, Fernig DG, Gherardi E, Gallagher JT, Pavao MS, Lyon M, Interactions of hepatocyte growth factor/scatter factor with various glycosaminoglycans reveal an important interplay between the presence of iduronate and sulfate density, J Biol Chem 283(9) (2008) 5235–48. [PubMed: 18156180]

[47]. Ito Y, Correll K, Schiel JA, Finigan JH, Prekeris R, Mason RJ, Lung fibroblasts accelerate wound closure in human alveolar epithelial cells through hepatocyte growth factor/c-Met signaling, Am J Physiol Lung Cell Mol Physiol 307(1) (2014) L94–105. [PubMed: 24748602]

[48]. Myerburg MM, Latoche JD, McKenna EE, Stabile LP, Siegfried JS, Feghali-Bostwick CA, Pilewski JM, Hepatocyte growth factor and other fibroblast secretions modulate the phenotype of human bronchial epithelial cells, Am J Physiol Lung Cell Mol Physiol 292(6) (2007) L1352–60. [PubMed: 17307814]

[49]. Warburton D, Bellusci S, The molecular genetics of lung morphogenesis and injury repair, Paediatr Respir Rev 5 Suppl A (2004) S283–7. [PubMed: 14980285]

[50]. Chakraborty S, Chopra P, Hak A, Dastidar SG, Ray A, Hepatocyte growth factor is an attractive target for the treatment of pulmonary fibrosis, Expert Opin Investig Drugs 22(4) (2013) 499–515.

[51]. Hitchcock AM, Yates KE, Costello CE, Zaia J, Comparative glycomics of connective tissue glycosaminoglycans, Proteomics 8(7) (2008) 1384–97. [PubMed: 18318007]

[52]. Lee HY, Han L, Roughley PJ, Grodzinsky AJ, Ortiz C, Age-related nanostructural and nanomechanical changes of individual human cartilage aggrecan monomers and their glycosaminoglycan side chains, J Struct Biol 181(3) (2013) 264–73. [PubMed: 23270863]

Highlights:

- Lung decellularization results in differential loss of glycosaminoglycans (GAGs)
- Specific sulfation patterns of GAGs are differentially depleted
- Remaining GAGs are unable to bind key matrix-associated growth factors
- Combination of GAGs and matrix-associated growth factors differentially effects growth of three different types of lung cells cultured on or embedded within decellularized human lung gels

Statement of Significance

Despite progress in use of decellularized lung scaffolds in ex vivo lung bioengineering schemes, including use of gels and other materials derived from the scaffolds, the detailed composition and functional role of extracellular matrix (ECM) proteoglycans (PGs) and their glycosaminoglycan (GAG) chains remaining in decellularized lungs, is poorly understood. In the current studies, we demonstrate that glycosaminoglycans (GAGs) are significantly depleted during decellularization and those that remain are dysfunctional and unable to bind matrix-associated growth factors critical for cell growth and differentiation. Systematically repleting GAGs and matrix-associated growth factors to gels derived from decellularized human lung significantly and differentially affects cell growth. These studies highlight the importance of considering GAGs in decellularized lungs and their derivatives

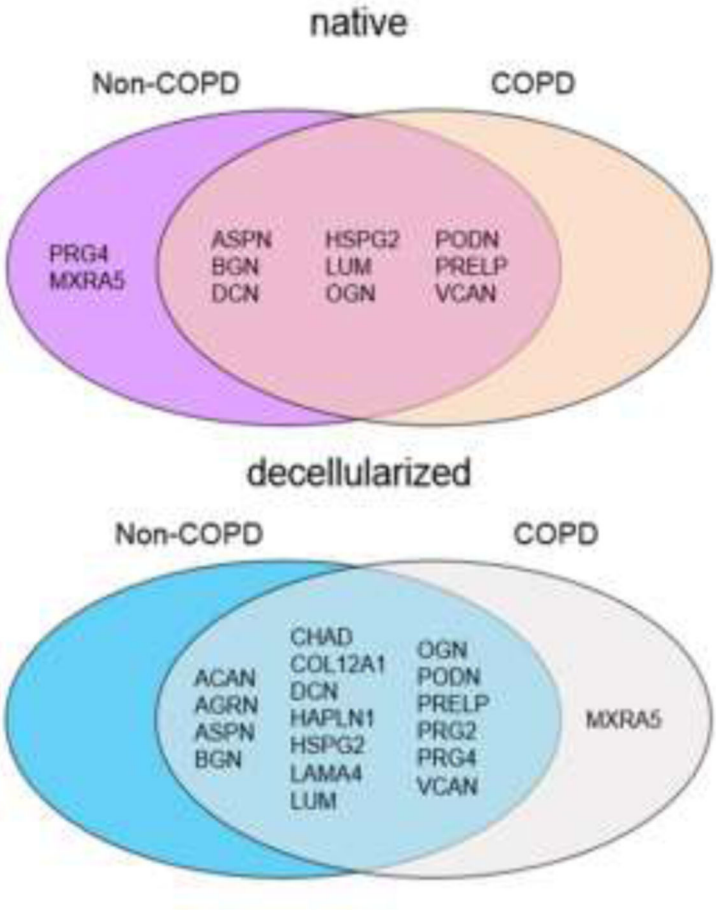

ACAN	Aggrecan
AGRN	Agrin
AMBP	Protein AMBP
ASPN	Asporin
BGN	Biglycan
CHAD	CD44 antigen
CD74	Chondroadherin
COL12A1	Collagen alpha-1(XII)
COL15A1	Collagen alpha-1(XV)
DCN	Decorin
HAPLN1	Hyaluronan and proteoglycan link protein 1
HSPG2	Basement membrane-specific heparan sulfate proteoglycan core protein
LAMA4	Laminin subunit alpha-4
LUM	Lumican
MXRA5	Matrix-remodeling-associated protein 5
OGN	Mimecan
PODN	Podocan
PRELP	Prolargin
PRG2	Bone marrow proteoglycan
PRG4	Proteoglycan 4
VCAN	Versican

Figure 1: The detection of proteoglycans is comparable in native and decellularized non-COPD and COPD human lungs.

Overlap of proteoglycan proteins in native and decellularized tissue from non-COPD and COPD patients. Data reflects one each of native non-COPD or COPD and pooled data from 3 decellularized COPD and 8 decellularized non-COPD lungs.

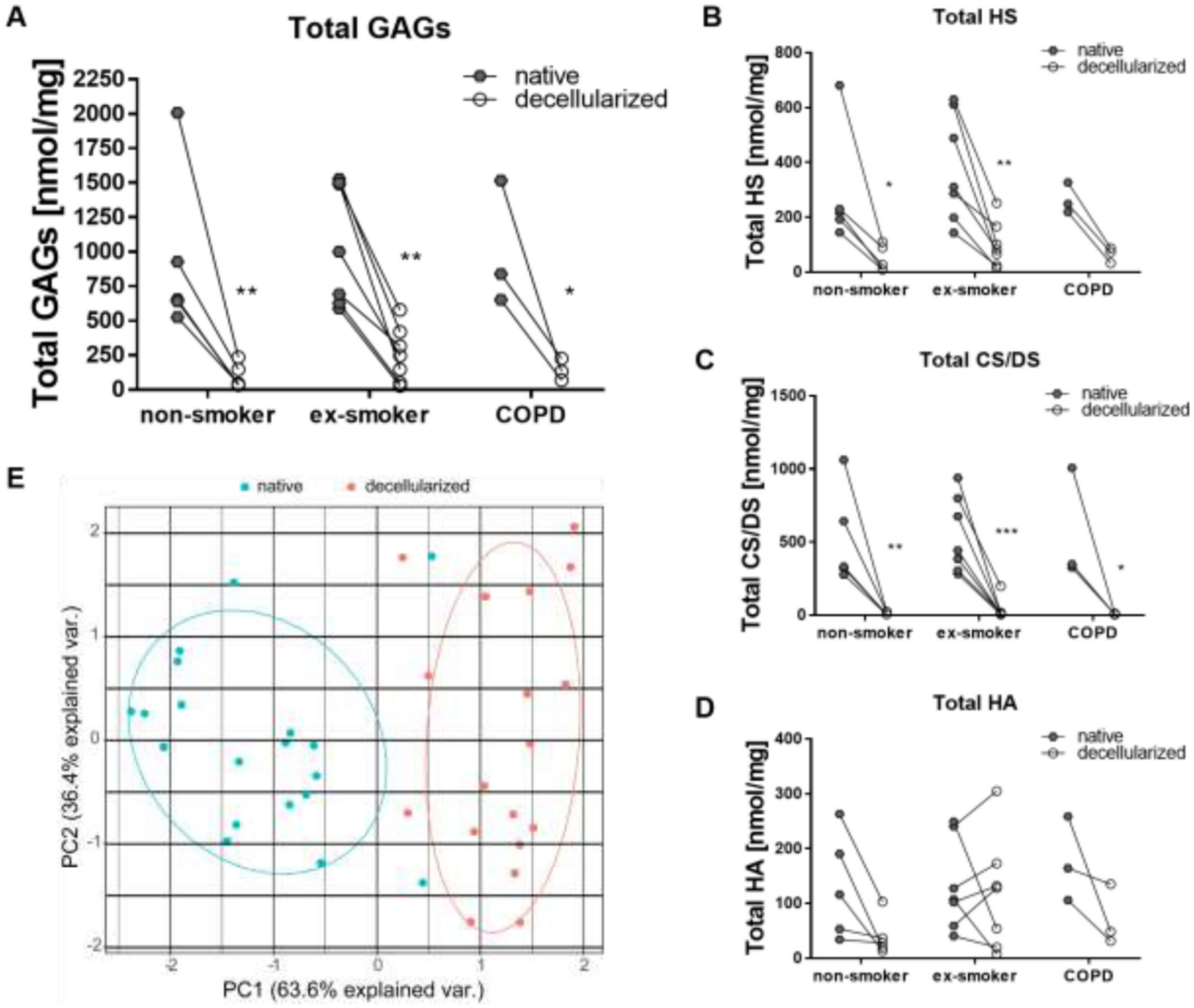

Figure 2: Paired comparison of glycosaminoglycan (GAG) amount in native and decellularized tissue from non-smokers, ex-smokers, and COPD patients shows no significant difference between the three different groups.

Total amount of GAGs (A), heparan sulfate (HS) (B), chondroitin sulfate/dermatan sulfate (CS/DS) (C), and hyaluronic acid (HA) (D). E) Principal component analysis of GAG content demonstrates segregation between native and decellularized human lungs. Results from 5 non-smoker, 7 ex-smoker, and 3 COPD lungs are depicted.

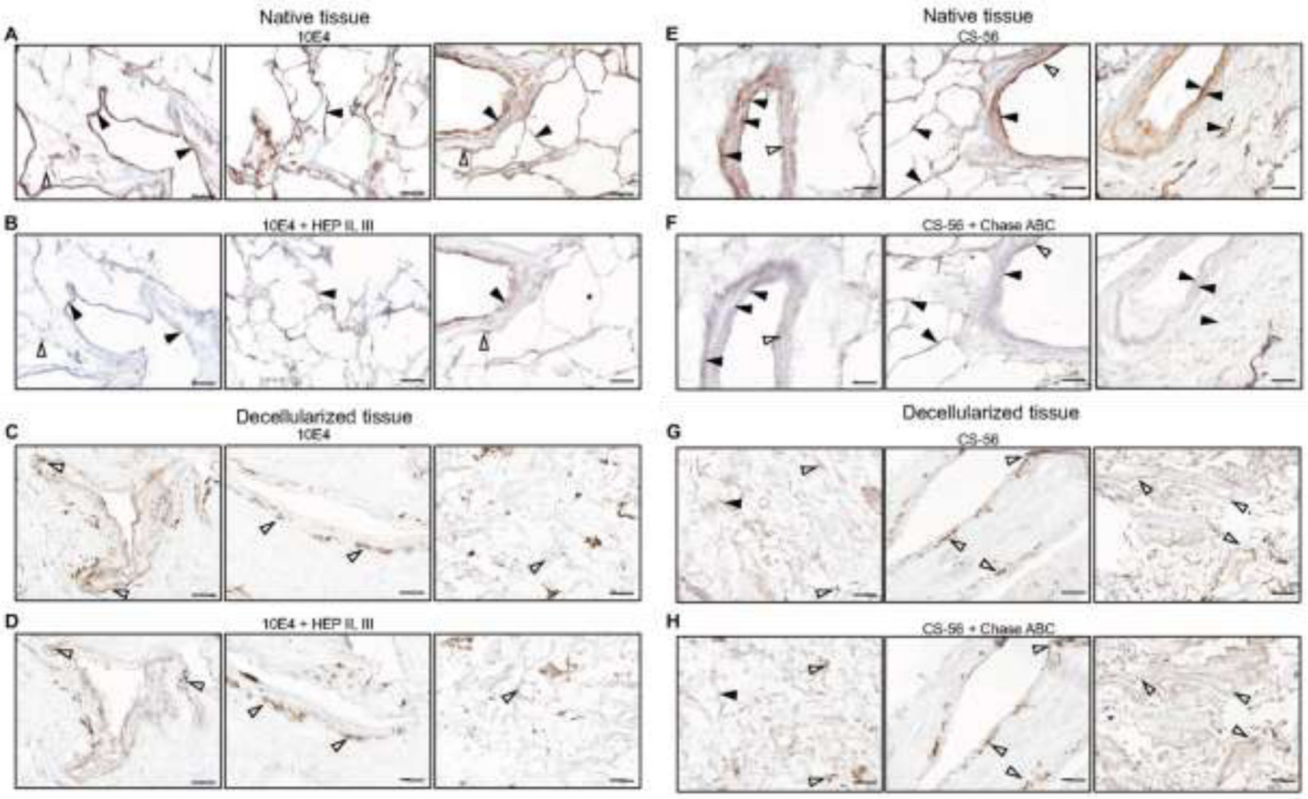

Figure 3: HS and CS/DS are absent in decellularized lungs.

Immunohistochemical staining of heparan sulfate (HS) (A-D) and of chondroitin sulfate/dermatan sulfate (CS/DS) (E-H) in native and decellularized lungs from a non-COPD patient. For HS the 10E4 antibody was used and to control the specificity of the staining sequential sections were pretreated with heparinase II and III (B, D) that abolish the HS epitopes. Solid arrowheads show heparinase-sensitive staining while open arrowheads show unspecific heparinase-insensitive staining. For CS/DS the CS-56 antibody was used and in this case chondroitinase ABC pretreatment (F, H) was used to control the staining specificity. Solid arrowheads show chondroitinase ABC-sensitive staining while open arrowheads show unspecific chondroitinase ABC-insensitive staining. Scale bars = 100 μm.

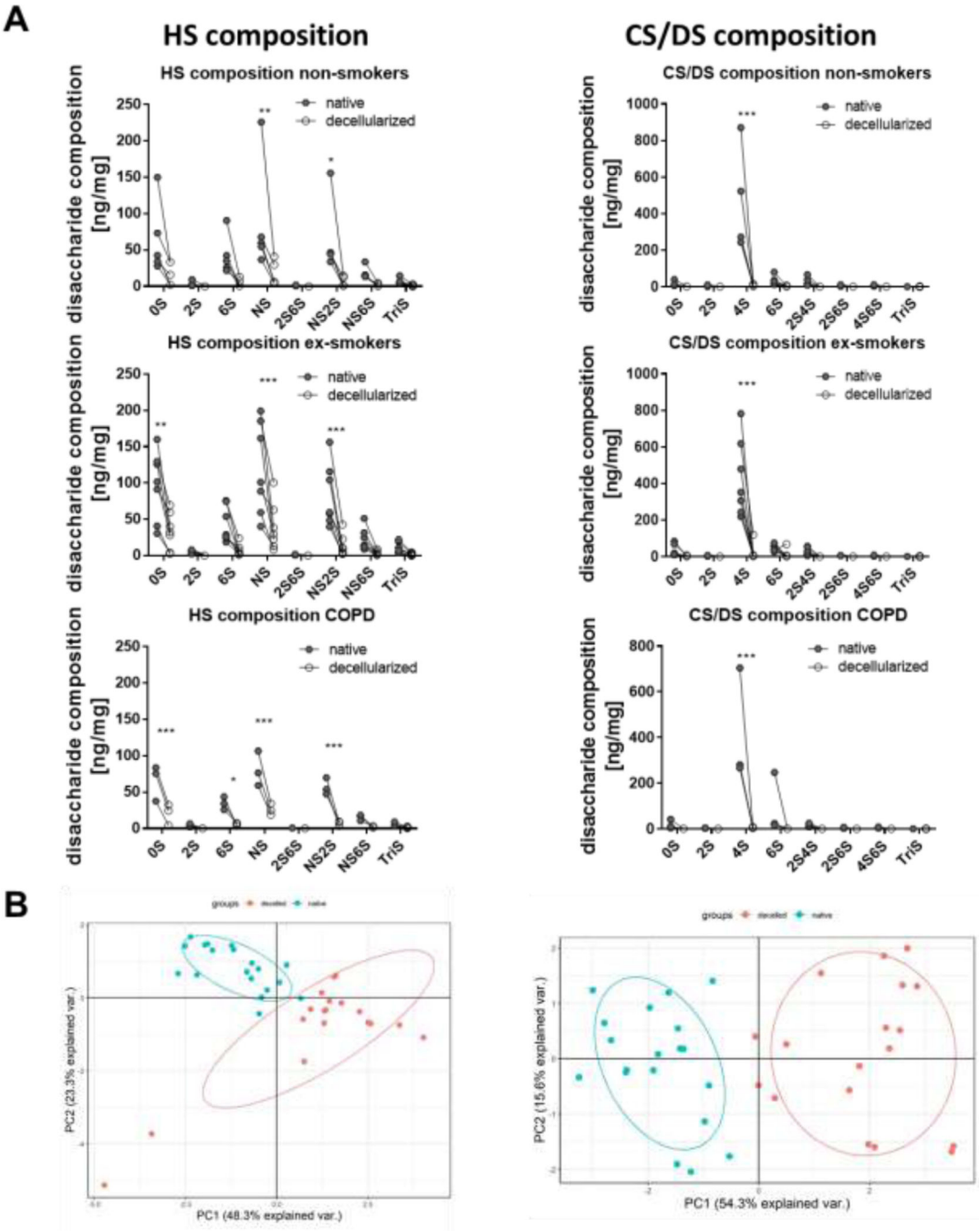

Figure 4: Quantification of heparan sulfate (HS) and chondroitin sulfate/dermatan sulfate (CS/DS) composition in native and decellularized non-COPD and COPD tissue.

A) Total amount of HS and CS/DS side chains. B) Principal component analysis of HS and CS/DS composition demonstrates segregation between native and decellularized (decelled) human lungs. Results from 5 non-smokers, 7 ex-smokers, and 3 COPD lungs are depicted. Abbreviations HS graphs: UA-GlcNAc, 0-sulfated (S) = nonsulfated disaccharide, where UA is deoxy-α-L-threo-hex-4-enopyranosyluronic acid and GlcNAc is N-acetylglucosamine; UA2S-GlcNAc, 2S = 2-sulfated disaccharide; UA-GlcNS, NS = N-sulfated disaccharide; UA-GlcNAc6S, 6S = 6-sulfated disaccharide; UA2S-GlcNAc6S,

2S6S = 2, 6-disulfated disaccharide; UA-GlcNS6S, NS6S = N-sulfated, 6-sulfated disaccharide; UA2S-GlcNS, NS2S = N-sulfated 2-sulfated disaccharide; UA2S-GlcNS6S, TriS = trisulfated disaccharide. Abbreviations CS/DS graphs: UA-GalNAc, 0-sulfated (S) = nonsulfated disaccharide, where UA is deoxy-α-L-threo-hex-4-enopyranosyluronic acid and GalNAc is N-acetylgalactosamine; UA2S-GalNAc, 2S = 2-sulfated disaccharide; UA-GalNAc4S, 4S = 4-sulfated disaccharide; UA-GalNAc6S, 6S = 6-sulfated disaccharide; UA-GalNAc4S,6S, 4S6S = 4, 6-disulfated disaccharide; UA2S-GalNAc4S, 2S4S = 2, 4-disulfated disaccharide; UA2S-GalNAc6S, 2S6S = 2, 6-disulfated disaccharide; UA2S-GalNAc4S6S, TriS = trisulfated disaccharide.

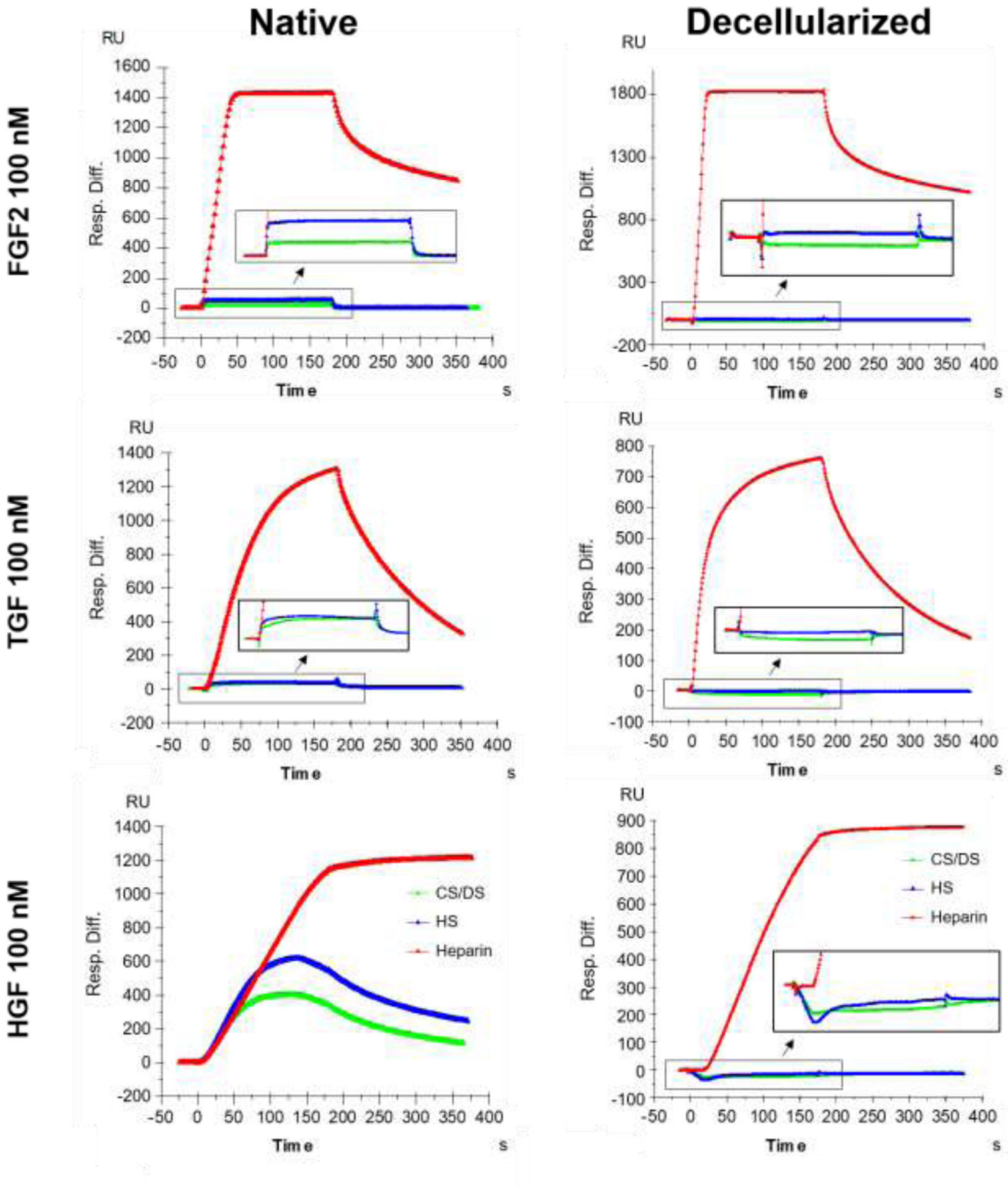

Figure 5: Key matrix-associated growth factors (fibroblast growth factor (FGF2), hepatocyte growth factor (HGF), and transforming growth factor beta (TGFβ1)) do not bind to glycosaminoglycans (GAGs) isolated from decellularized non-COPD human lung extracellular matrix (ECM) homogenates.

Surface plasmon resonance analysis of the binding of 100 nM FGF2, HGF, and TGFβ1 was assessed in heparan sulfate (HS) and chondroitin sulfate/dermatan sulfate (CS/DS) isolated from 3 native and 3 decellularized non-COPD lung tissues. Representative graphs are shown from an individual lung. Heparin served as positive control for binding.

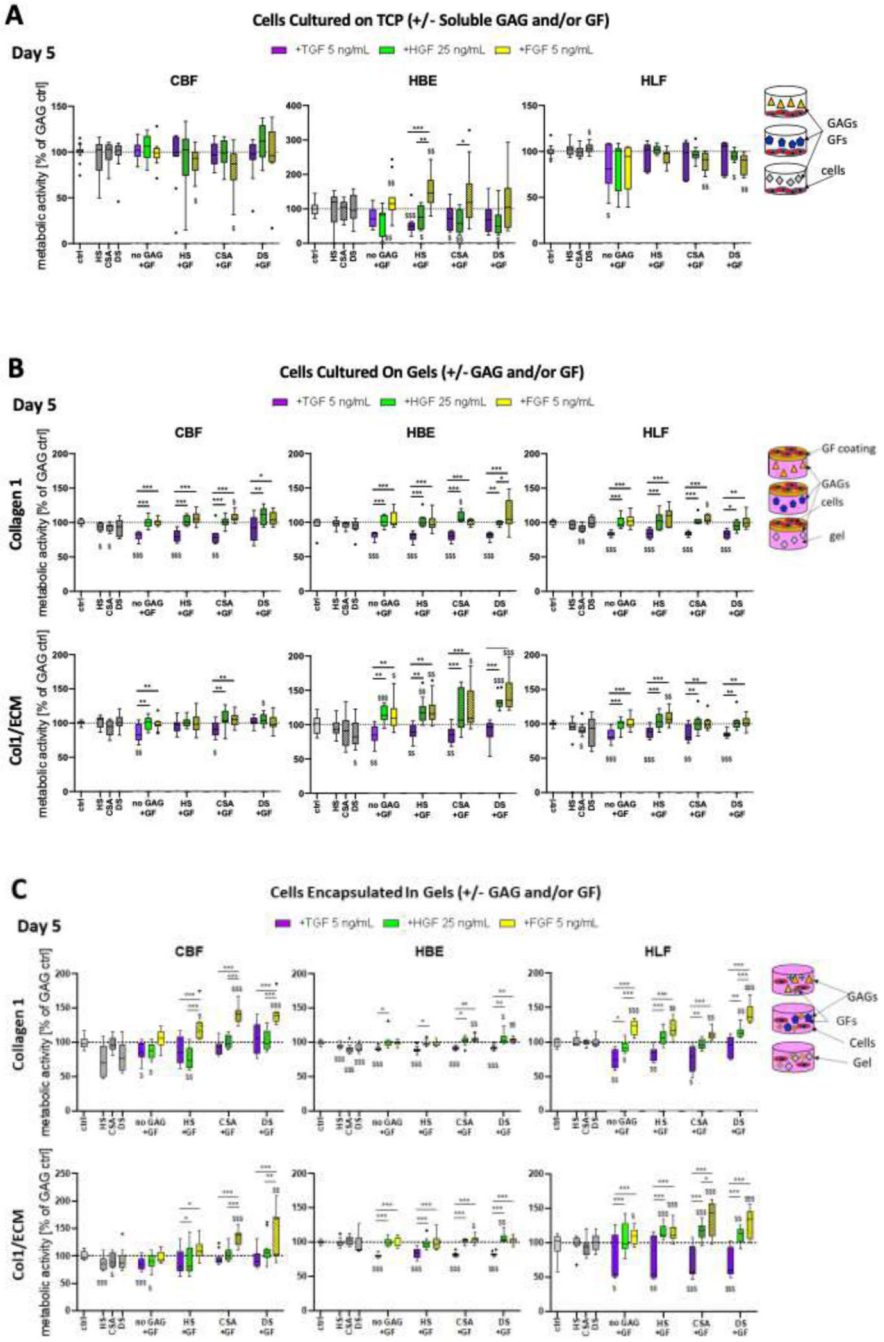

Figure 6 (A): Glycosaminoglycans (GAGs) in combination with matrix-associated growth factors and method of cultivation differentially influences metabolic activity of human pulmonary vascular endothelial cells (CBF), human bronchial epithelial cells (HBE), and human lung fibroblasts (HLF).

A) Metabolic activity of CBF, HBE, and HLF cells grown for 5 days on tissue culture plastic (TCP) with addition of GAGs (1 μM) in combination with different matrix-associated growth factors (TGFβ1, HGF, FGF2) into the cultivation medium. Combined data from 3 experiments with n=3–4 replicates each. (B) Metabolic activity of CBF, HBE, and HLF cells cultured on top of type I collagen (Col1) or human lung ECM/type I collagen hybrid gels

(Col1/ECM), prepared with addition of GAGs (HS, CSA, or DS @ 5 μM) and/or surface treated with growth factors (TGFβ1, HGF, FGF2); and (C) Metabolic activity of the same cell lines encapsulated within collagen 1 or Col1/ECM gels, with GAGs (HS, CSA, or DS @ 5 μM) and/or growth factors added within the gels. The data from the addition of GAGs only and growth factors only (+HS, +CSA, +DS, +TGF, +HGF, +FGF) was normalized to the control (= medium without GAG or growth factor addition). Metabolic activity of the combination treatments (GAG+GF) was normalized to the respective GAG without addition of GF. $: significant to control (dotted line, one-sample t-test). *: significant within group (One-way ANOVA). $ $ $,***=p<0.001, $ $,**=p<0.01, $,*=p<0.05. Combined data from gels from 3 experiments with n=4 replicates each. The dotted line represents pure gels without addition of GAGs or matrix-associated growth factors.

Table 1:
Patient demographics for the lungs utilized in this study.

Smoking, clinical, and radiographic history obtained as available from post-mortem chart review.

Lung #	Age	Sex	Smoking history	Pulmonary history
Non-COPD				
1	72	M	lifelong non-smoker	none
2	93	F	lifelong non-smoker	acute pulmonary embolism at time of death
3	82	F	lifelong non-smoker	none
4	58	M	ex-smoker	acute pulmonary embolism at time of death
5	59	M	ex-smoker, 25Pky	none
6	83	F	lifelong non-smoker	none
7	83	F	ex-smoker, quit 47 years prior to death	none
8	65	M	lifelong non-smoker	none
9	77	F	lifelong non-smoker	none
10	73	M	ex-smoker, quit 49 years prior to death	none
11	80	M	ex-smoker, quit 36 years prior to death	none
12	64	F	ex-smoker, 28Pky, quit 20 years prior to death	none
13	60	F	lifelong non-smoker	none
14	84	F	lifelong non-smoker	acute lobar pneumonia at time of death (non-involved lobe used)
15	61	M	ex-smoker quit 2 years prior to death	respiratory bronchiolitis on chest CT
16	65	M	lifelong non-smoker	none
17	42	M	ex-smoker 1 PPD quit 4 years prior to death	none
COPD				
1A, 1B (2 lobes)	74	M	ex-smoker, 50Pky, quit 17 years prior to death	clinical diagnosis of COPD
2	72	M	current smoker	centroacinar emphysema
3	75	M	ex-smoker, 22Pky, quit 36 years prior to death	centroacinar emphysema
4	57	M	current smoker, 1pack per day	centroacinar emphysema

M: male, F: female, Pky: pack years, CT: computer tomography.

Table 2:

Summarized patient demographics for the lungs utilized in this study.

Disease state	Age	Sex M/F	Time to autopsy [h]	Smoking history never/ex/current
Non-smokers	75.7 ± 10.9	3/6	61.1 ± 18.7	9/0/0
Ex-smokers	65.0 ± 13.3	6/2	37.3 ± 32.8	0/8/0
COPD	69.5 ± 8.4	5/0	29.6 ± 18.9	0/3/2

M: male, F: female.

Table 3:

Summary of the differential effects of glycosaminoglycans (GAGs) and/or growth factor addition on metabolic activity of human pulmonary vascular endothelial cells (CBF), human lung epithelial cells (HBE), and human lung fibroblasts (HLF) at different culture conditions when normalizing the data to the respective GAG without addition of growth factor.

TCP: Tissue culture plastic, Col 1: type 1 collagen, Col1/ECM: human lung ECM/type 1 collagen.

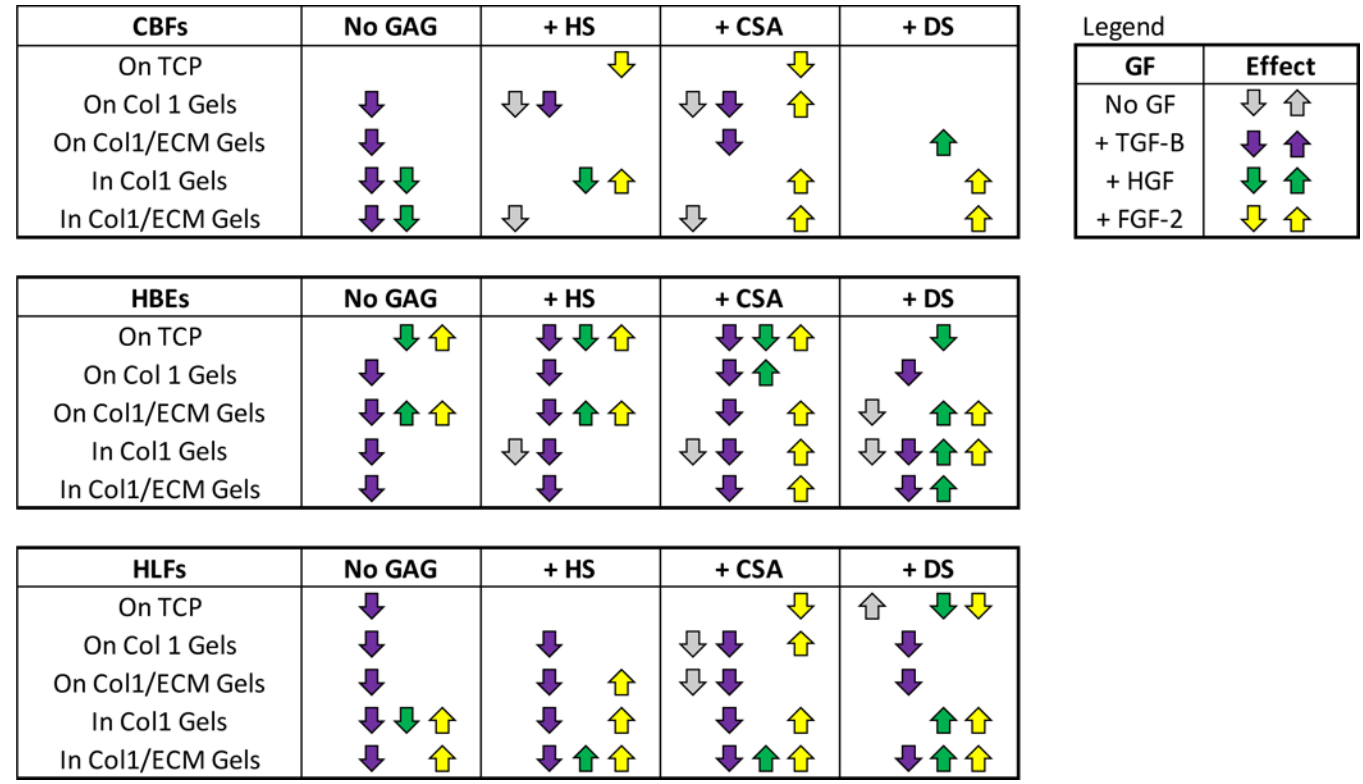

Table 4:

Summary of the differential effects of glycosaminoglycans (GAGs) and/or growth factor addition on metabolic activity of human pulmonary vascular endothelial cells (CBF), human lung epithelial cells (HBE), and human lung fibroblasts (HLF) at different culture conditions when normalizing the data to the respective growth factor without addition of GAG.

TCP: Tissue culture plastic, Col 1: type 1 collagen, Col1/ECM: human lung ECM/type 1 collagen.